AD_____

Award Number: W81XWH-11-1-0628

TITLE: Targeting Transforming Growth Factor Beta to Enhance the Fracture Resistance of Bone

PRINCIPAL INVESTIGATOR: Jeffry S. Nyman

CONTRACTING ORGANIZATION: Vanderbilt University, Nashville, TN 37240-7830

REPORT DATE: January 2013

TYPE OF REPORT: Final

PREPARED FOR: U.S. Army Medical Research and Materiel Command
Fort Detrick, Maryland 21702-5012

REPORT DOCUMENTATION PAGE

Form Approved
OMB No. 0704-0188

1. REPORT DATE	2. REPORT TYPE	3. DATES COVERED
January 2013	Final	15 July 2011 – 14 December 2012

4. TITLE AND SUBTITLE

Targeting Transforming Growth Factor-beta to Enhance the Fracture Resistance of Bone

5a. CONTRACT NUMBER

5b. GRANT NUMBER
W81XWH-11-1-0628

5c. PROGRAM ELEMENT NUMBER

6. AUTHOR(S)
Jeffry S. Nyman

E-Mail: jeffry.s.nyman@vanderbilt.edu

5d. PROJECT NUMBER

5e. TASK NUMBER

5f. WORK UNIT NUMBER

7. PERFORMING ORGANIZATION NAME(S) AND ADDRESS(ES)
Vanderbilt University Medical Center

Nashville TN 37240-7830

8. PERFORMING ORGANIZATION REPORT NUMBER

9. SPONSORING / MONITORING AGENCY NAME(S) AND ADDRESS(ES)
U.S. Army Medical Research and Materiel Command
Fort Detrick, Maryland 21702-5012

10. SPONSOR/MONITOR'S ACRONYM(S)

11. SPONSOR/MONITOR'S REPORT NUMBER(S)

12. DISTRIBUTION / AVAILABILITY STATEMENT
Approved for Public Release; Distribution Unlimited

13. SUPPLEMENTARY NOTES

14. ABSTRACT

Because aging can lower the fracture resistance of bone in ways that are independent of bone mass, the present project investigated the possibility that transforming growth factor (TGF)-Beta inhibition could improve multiple measurements of fracture resistance in growing, mature adult, and old rodents. TGF-Beta inhibition was achieved with a neutralizing antibody known as 1D11. When administered to growing mice for 4 weeks (13 to 17 weeks of age), 1D11 substantially increased trabecular bone volume fraction. Moreover, treatment-related improvements in trabecular architecture and tissue mineral density translated to stronger vertebral bodies. When administered to adult (6 months) and old rats (22 months) for 6 weeks, 1D11 did not have an appreciable effect on trabecular bone. As another example of differential effects of 1D11 between mice and rats, treatment increased the estimated material strength of cortical bone in mice while it increased the structural strength of cortical bone in old rats with no effects on bone in adult rats. In comparison to control antibody treatment, 1D11 also increased the fracture toughness of bone from growing mice and old rats. These effects appear to be independent of bone mass, and identifying the cause (e.g., changes in collagen crosslinking) is the next step.

15. SUBJECT TERMS
Fracture resistance, Osteoporosis, Biomechanics

16. SECURITY CLASSIFICATION OF:			17. LIMITATION OF ABSTRACT	18. NUMBER OF PAGES	19a. NAME OF RESPONSIBLE PERSON
a. REPORT	b. ABSTRACT	c. THIS PAGE			USAMRMC
U	U	U	UU		19b. TELEPHONE NUMBER *(include area code)*

Table of Contents

	Page
Introduction……..…….…..	**2**
Body…….	**2**
Key Research Accomplishments……..	**6**
Reportable Outcomes……	**6**
Conclusion……	**7**
References……	**7**
Appendices……	**8**

INTRODUCTION:

As women and men age, the likelihood of suffering a fracture increases [1]. Since this increase in fracture risk is not solely explained by an age- or menopausal-related decrease in bone mass [2,3], new anti-fracture therapies should also address other determinants of fracture resistance besides bone mass to be effective. One promising target is transforming growth factor-beta, a relatively abundant protein in bone that influences osteoblast differentiation as well as the extracellular matrix [4]. Thus, the goal of this CDMRP project, entitled *Targeting Transforming Growth Factor Beta to Enhance the Fracture Resistance of Bone* is to determine whether the suppression of TGF-β activity improves the fracture resistance independent of effects on bone mass in rodents of varying age including very old rats with compromised bone quality.

BODY:

Preliminary work to establish effectiveness of neutralizing antibody

Prior to conducting the rat study, we needed to ensure that our batch of the anti-TGF-β antibody (2G7) from the Vanderbilt Antibody and Protein Resource Laboratory sufficiently neutralized TGF-β and caused the expected effect on bone. To do so, we conducted a head-to-head study in which 13-week-old male, FVB mice were treated for 4 weeks with intraperitoneal injections (i.p.) of either 2G7 at 1 of 2 doses (10 mg/kg and 20 mg/kg) or 1D11 from Genzyme Corporation (A Sanofi Company) at a dose previously determined to be effective in 13-week-old male, C57/BL6 mice (10 mg/kg) [5]. Respective control antibodies (12CA5 and 13C4) were included. We used *ex vivo* micro-computed tomography (μCT) scans at an isotropic voxel size of 12 μm to assess the effect of treatment on the amount of trabecular bone (BV/TV) within the femur metaphysis. To our surprise, only 1D11 significantly increased BV/TV of the femur metaphysis (Figure 1). A subsequent *in vitro* TGF-β reporter assay confirmed that 2G7 reduced SMAD2 signaling (downstream effector) in a transfected human cancer cell line by only 20%, whereas 1D11 reduced downstream signaling by 90%, further establishing that our 2G7 was ineffective. Therefore, in subsequent studies, we used 1D11, which was kindly donated by Genzyme through a Material Transfer Agreement between the company and Vanderbilt University. Unfortunately, getting the agreement in place delayed the rat experiment.

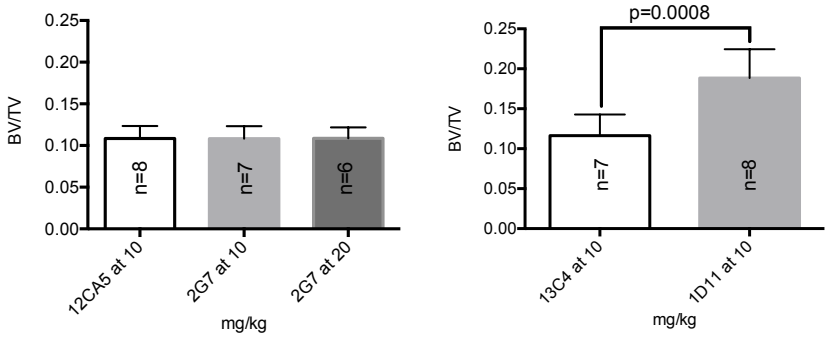

Figure 1. The locally supplied anti-TGF-β antibody 2G7 did not increase trabecular bone fraction in the femur metaphysis (Left) as determined by a one-way ANOVA; whereas a commercially supplied antibody 1D11 did (Right) as determined by a two-sided Student's t-test. (mean ± SD)

Establishing a tool for predicting strength of mouse vertebral bodies

Since the goal of this CDMRP project is to fully characterize fracture resistance, we used the 1D11-arm of the male mouse study to develop a non-destructive computational tool – known as μCT-derived finite element analysis (FEA) – for predicting vertebral body (VB) strength. CT-FEA can accurately assess the contribution of bone architecture to fracture resistance and is now being using in clinical studies of fracture [6]. Our μCT-FEA research will be presented at the upcoming 2013 Orthopaedic Research Society Meeting (see abstract in the Appendix for details on the technique and findings). Briefly, for the first time using mouse VBs, we showed that a simple modification to an existing elastic failure criteria [7] could predict VB strength, as determined by compression testing, and that 1D11 treatment increased VB strength primarily through increase in bone volume fraction but with some contribution from a treatment-related increase in tissue mineral density. This newly validated technique allows us and others to non-destructively determine the contribution of bone architecture and structure to whole bone strength such that the same specimens can subsequently be used for histology based mechanistic studies, thereby allowing more efficient and rapid progress in the field.

Effect of TGF-β suppression on fracture resistance in rats

To test our working hypothesis that an antibody targeted against TGF-β increases the fracture resistance of young and aged bone by enhancing bone tissue-level properties, not just bone mass, young (6 months) or old

(22 months) male, Fischer F344 rats from the National Institute on Aging (NIA) were treated with the 13C4 control antibody or the 1D11 antibody at 1 or 5 mg/kg (1D11-1 or 1D11-5 groups, respectively; these recommended doses from Genzyme were based on their own ovariectomy rat studies) (Task 2). Injections were given i.p. at a frequency of 3 times per week for 6 weeks. Following an IACUC-approved protocol (Task 1), rats were euthanized, and all long bones were harvested. Throughout the 2-week acclimation period and 6-week treatment period, the young adult rats gained body weight while the old rats lost it. Per IACUC protocol, 3 of 36 rats were euthanized before treatment began because their body weight dropped below 20% of the baseline weight. After treatment commenced, 1 of 11 rats in the 13C4 group, 2 of 10 rats in the 1D11-1 group, and 2 of 12 rats in the 1D11-5 group were euthanized before completion of the study. The bones from these rats were not analyzed resulting in the following final n for each group: n=10 (13C4), n=8 (1D11-1), and n=10 (1D11-5). Since the young adult rats gained weight, none of these animals were removed, leaving the intended n=12 rats per treatment. µCT with 10 µm voxel size (Task 3a) quantified cortical (I_{min}) and trabecular (BV/TV) parameters as well as tissue mineralization density (TMD) [8], and three-point bend testing of un-notched radius (Task 3b) [9] and notched femur (Task 3d) quantified strength and fracture toughness of the long bones, respectively. For details on the notching method and fracture toughness calculation, see the abstract in the appendix that was presented at the 2012 American Society for Bone and Mineral Research (ASBMR) Annual Meeting.

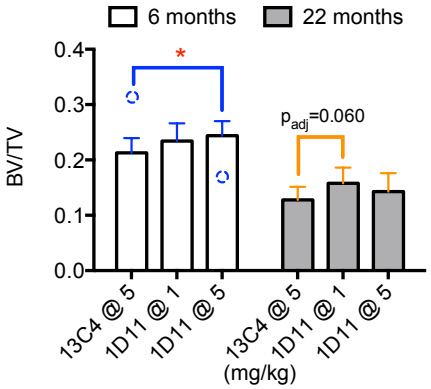

*Figure 2. 1D11 at the higher dose only increased trabecular bone volume fraction in the femur metaphysis of young adult rats after removing outliers (mean ± SD with p-values adjusted by Holm-Sidak method for multiple pair-wise comparisons within age group; *p<0.05).*

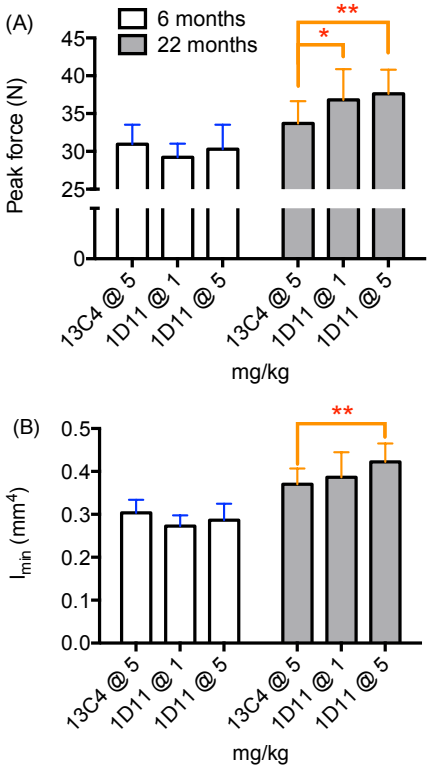

*Figure 3. 1D11 increased the whole bone strength in bending of the radius from only old rats (A), and this in explained in part by an increase in treatment-related increase in cortical bone structure (mean ± SD with p-values adjusted by Holm-Sidak method for multiple pair-wise comparisons within age group; **p<0.01).*

Unlike the developing young, male FVB mice, 1D11 treatment did not have a demonstrative effect on the bone volume fraction (BV/TV) or trabecular architecture within the metaphysis of the femur from mature male F344 rats. Only when 2 outliers (2 standard deviations away from mean) were removed did a two-way ANOVA find a treatment effect (Figure 2). As expected, there was a clear difference in BV/TV between young and old rats, irrespective of treatment (ANOVA p<0.0001). While there was not much of a treatment effect on trabecular bone, suppression of TGF-β by 1D11 increased the whole bone strength of the radius (Figure 3A). However, this increase in the peak force endured by the cortical bone was only statistically significant in old rats. This increase could be explained by a treatment-related increase in the moment of inertia (I_{min}) of the radius mid-shaft (Figure 3B), where I_{min} measures the distribution of tissue about the neutral bending axis (structure). Likewise, structural strength of the radius was likely higher for the old rats than for young rats because I_{min} increased with aging. When we factored out the contribution of structure to whole bone strength using the flexure equation [8], there were no statistically significant differences in estimated material strength among the treatment groups (AVOVA p=0.139; Figure 4A), this lack of a treatment effect could be due to a lack of a difference in tissue mineral density (TMD) among the treatment groups (ANOVA p=0.0896; Figure 4B). Interestingly, while TMD was clearly higher for old bone (Figure 4B), the bone from the old rats was not stronger than the bone from the young adult rats. Although 1D11 treatment had no effect on estimated material strength overall, it tended to reverse the age-related loss in strength, especially at the low dose (13C4-5 vs. 1D11-1, $p_{adj.}$=0.0522 within 22 months of age). However, this effect cannot be explained by treatment-related increase in TMD.

Besides structural and material strength, fracture resistance also depends on the ability of the tissue to dissipate energy during failure such that brittle bones have poor energy dissipation. Therefore, we tested for

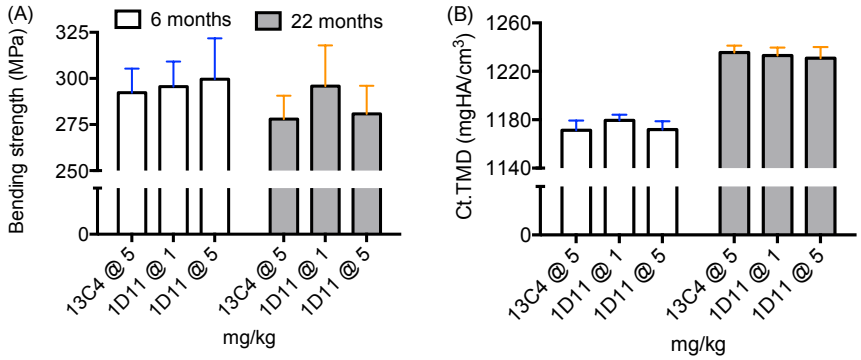

Figure 4. Suppression of TGF-β by 1D11 did not improved estimated material strength (A) or tissue mineral density (B) of the radius in either young or old rats, although there was a non-significant trend of 1D11 at the lower dose reversing age-related loss in strength. (mean ± SD).

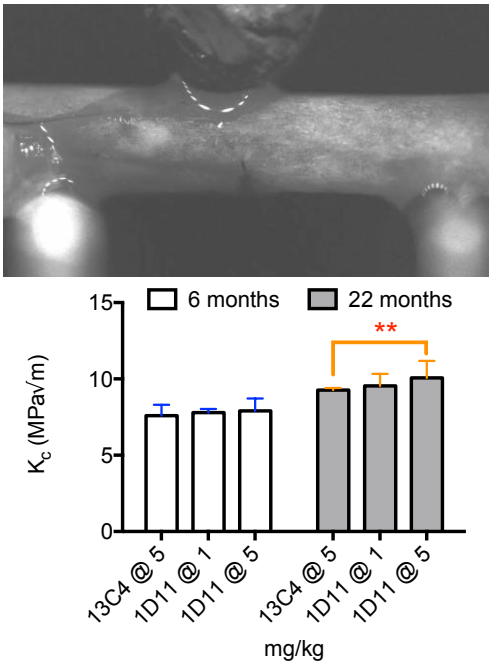

Figure 5. When loading a notched femur in three-point bending, a crack propagates from the posterior to the anterior side of the femur mid-shaft (Above). By this test, 1D11 was found to increase fracture toughness in old rats. (mean ± SD with p-values adjusted by Holm-Sidak method for multiple pair-wise comparisons within age group;

differences in post-yield deflection (PYD: amount of deformation after yield or the onset of permanent damage), toughness (U_t: energy-to-failure normalized to bone cross-sectional area), and fracture toughness (K_c: resistance to crack propagation). PYD and U_t was assessed from three point bending of the radii. As determined by a two-way ANOVA, there were no differences in post-yield deflection or in toughness among the treatment groups (PYD: $p=0.996$ and U_t: $p=0.763$), but there were differences between the age groups (PYD: $p<0.0001$ and U_t: $p<0.0001$). Thus, bones become brittle with age in the male F344 rats, and 6 weeks of 1D11 did not reverse this effect. Interestingly, when we created a notch in the femur and then tested the bone in three-point bending to propagate a crack, 1D11 treatment was found to increase the ability of the cortical tissue to resist crack propagation (Figure 5). However, as revealed in the post-hoc analysis, this effect primarily occurred in the old rats.

Effect of TGF-β suppression on fracture resistance in female mice

Since the suppression of TGF-β activity by 1D11 did not affect the fracture resistance of young adult male rats as expected from our previously published research [5,10] and our unpublished work involving mice (see abstracts in appendix), we decided to verify that the new batch of 1D11 antibody from Genzyme was effective (i.e., not inadvertently denatured by freeze-thaw cycles or some unknown handling procedure). Therefore, we repeated the aforementioned 13 week, male FVB mice study (Figure 1) in 13 week, female FVB mice using the same aliquots of the antibody that was administered to the male rats. The reasons for testing the effect of 1D11 on bone in female FVB mice were four fold: the importance of preventing fractures among women; there is already published data on the effect of 1D11 on bone in male mice, but not in females; FVB mice have a higher baseline BV/TV and TMD than the C57BL6 strain [11]; and their femurs snap when subjected to bending making assessment of toughness possible, whereas C57BL6 bones exhibit excessive deformation and do not often snap.

To ensure sufficient power for detecting treatment effects on biomechanical properties of bone (not just BV/TV), we administered 13C4 at 10 mg/kg to 13 female mice and 1D11 at 10 mg/kg to 12 female mice, beginning at 13-weeks of age. As was done in the previous mouse studies, the i.p. injections were given 3 times per week for 4 weeks (Task 2). Thus, we euthanized the mice at 17 weeks of age, which corresponds to the end of the growth phase. The same methods were used to assess the effect of 1D11 on bone (Task 3).

Confirming that our batch of 1D11 is not necessarily ineffective, trabecular bone volume fraction was clearly greater in the femur metaphysis of 1D11-treated mice than that of 13C4-treated mice. Moreover, treatment improved trabecular architecture as determined by μCT-derived connectivity density (Conn.D) and TMD (Table 1). Since these changes, imply that the trabecular bone from treated mice is stronger than bone from non-treated mice, we also scanned the L6 vertebra (VB) by μCT and then tested them in compression to failure (monotonic loading)..The same treatment effects occurred for the trabeculae of the VB: greater BV/TV,

Table 1. Selected properties (mean ± SD) of trabecular and cortical mouse bone

Property	Units	13C4	1D11	p-value
Femur metaphysis		n=13	n=12	
BV/TV		0.092 ± 0.017	0.195 ± 0.042	<.0001
Conn.D.	mm^{-3}	91.6 ± 32.4	143.3 ± 30.6	0.0004
Tb.TMD	$mgHA/cm^3$	1015 ± 12	1047 ± 7	<.0001
Femur diaphysis				
I_{min}	mm^4	0.125 ± 0.016	0.121 ± 0.012	0.553
Ct.TMD	$mgHA/cm^3$	1289 ± 13	1286 ± 8	0.514
Peak force	N	21.9 ± 2.3	22.1 ± 1.5	0.784
PYD	mm	0.187 ± 0.082	0.158 ± 0.075	0.368

Conn.D, and TMD with 1D11 treatment (data not shown). More importantly, the VB strength was greater for the 1D11 treated female mice than the 13C4 treated female mice (see Figure 6 as well as ASBMR abstract in appendix).

Unlike trabecular bone architecture, the cortical bone structure of the diaphysis was not different between the 13C4 and 1D11 groups (Table 1). Being opposite of what we observed for the radius of the old rats, 1D11 treatment did not increase whole bone strength of the femur from young mice (Table 1) but did increase the estimated material strength (Figure 7). With regards to brittleness, there was no drug effect on PYD and toughness. However, the fracture toughness of femur mid-shaft was significantly, but marginally greater with 1D11 treatment (5.16 ± 0.59 vs. 5.61 ± 0.44; p=0.044 from a two-sided t-test). Interestingly, when scanned at an isotropic voxel size of 6 µm, instead of 12 µm, the notched, contralateral femurs in the 1D11 group had greater TMD than did the femurs in the 13C4 group (1339 ± 8 vs. 1329 ± 12, p=0.028). Lastly, we cultured bone marrow stromal cells from the humeri of all 25 female mice in osteogenic media. Providing some insight into the action of 1D11, the colony forming units expressing alkaline phosphatase (CFU-AP) was consistently lower for 1D11 treated mice than for the 13C4 treated mice. This suggests that 1D11 treatment depleted the osteoprogenitor pool to some extent as inhibition of TGF-β activity *in vivo* may favor osteoblast differentiation over cell renewal. For more information on molecular actions of TGF-β, see the article by my colleague Dr. Xiangli Yang and myself in the appendix.

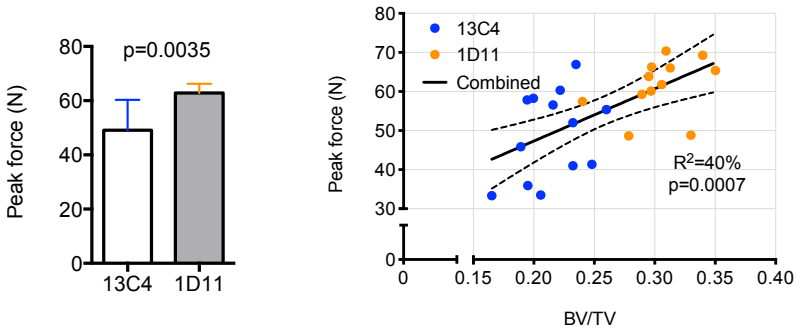

Figure 6. 1D11 increased mouse VB strength (Two-sided Student's t-test. mean ± SD), and this effect can be explained in part by an increase in trabecular bone volume fraction (Task 4c).

Unfulfilled tasks

While all demineralized tibia have been sectioned and stained (Task 3c) for bone histomorphometry, our previous, antiquated evaluation software kept crashing. Fortunately, after much waiting, the PI's local VA research office recently acquired a major upgrade to the microscope system and software (new camera, digital stage, and BIOQUANT software). Measurements of osteoblast and osteoclast numbers per bone surface are ongoing (Task 3f). The fatigue testing protocol of the ulna proved to be problematic (Task 3e). Following published methods [9], we ran the dynamic, three point bending tests in stress control in which the target force was calculated using the µCT-derived structural parameters. To our surprise, the young bones had much lower fatigue life than the old bones (no treatment). Since the young bones have lower stiffness than old bones, they were actually subjected to greater initial strain for the given stress than were the old rodent bones. Therefore, we are implementing a new protocol in which all bones are subject to the same initial strain. There will be several stress ranges as well. Quantifying

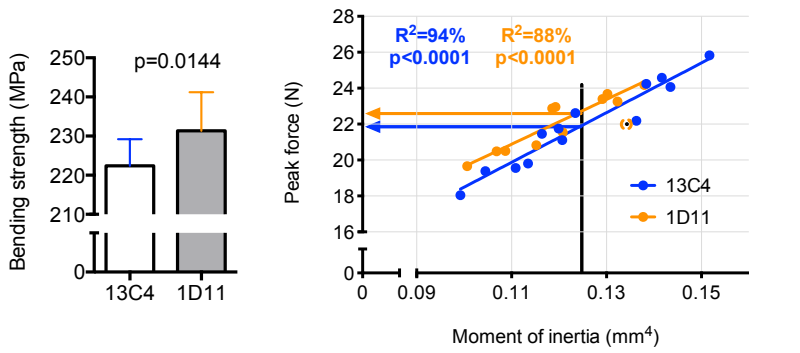

Figure 7. 1D11 increased estimated material strength of mouse cortical at the femur mid-shaft (Two-sided Student's t-test; mean ± SD). As a further check on this structure-independent effect, the y-intercept for the 1D11 regression line was greater than that for the 13C4 regression line (1 outlier removed).

collagen crosslinks by high performance liquid chromatography is the final unfilled task (3f). Despite performing this assay extensively as a postdoctoral fellow, the PI struggled mightily in setting up the assay at the VA with a different instrument. Despite this delay, we have observed that pentosidine, the non-enzymatic collagen crosslink biomarker, is higher in the old bone (24 month old rats) than in the young bone (6 month old rats). The next step is to determine whether 1D11 affects this crosslink as well as mature, enzymatic collagen crosslinks.

Planned future work

The PI has other resources to complete the unfilled tasks and perform 1 more rat study without additional funding. The plan is to submit the female mouse study for publication prior to the male rat study since it is closer to completion. Then, to address potential species dependency and age dependency, young 13 week old, F344 male rats will be treated with either 13C4 or 1 of 2 doses of 1D11 (as was done for the 6 month and 22 month old rats). If 1D11 increases BV/TV, we can conclude that TGF-β activity in trabecular bone is variable throughout the age of skeleton. If 1D11 does not increase BV/TV, then we can conclude that 1 mg/kg and 5 mg/kg are not particularly effective doses for affecting trabecular bone in rats, demonstrating an important species-specificity of this potential therapy. Alternatively, 6 weeks of treatment could be too long (mice were treated for only 4 weeks) or too short to observe an effect in rats. The effect of 1D11 on bone strength in young growing rats should also be equally interesting, and we can compare findings to what we have observed with our male and female mouse studies. Regardless of the outcomes, the work will be submitted to a journal.

KEY RESEARCH ACCOMPLISHMENTS:

- TGF-β inhibition is a target for increasing fracture resistance with effects beyond changing bone mass including improved trabecular architecture and material properties of cortical bone.
- The effectiveness of a neutralizing antibody to inhibit TGF-β is context dependent with differential effects on bone between young developing, mature adult, and aged rodents.
    - Trabecular bone of developing rodents, namely mice, is highly responsive to the anti-TGF-β antibody 1D11.
    - Whereas, 1D11 primarily affects cortical bone from aged rodents, namely rats.
- A tool for non-destructively assessing vertebral body strength was shown to reasonably match experimental measurements (destructive testing).

REPORTABLE OUTCOMES:

- Three abstracts at national society meetings
    - 2013 Orthopaedic Research Society Annual Meeting. San Antonio, TX. January 26-29.
      J.S. Nyman, A. Makowski, S. Uppuganti, J.A. Sterling, and D.S. Perrien. Assessing the Strength of Mouse Vertebral Bodies with μCT-derived Finite Element Analysis.
    - 2012 American Society for Bone and Mineral Research Annual Meeting. Minneapolis, MN. October 12-15.
      A.J. Makowski, S. Uppuganti, and **J.S. Nyman**. Measuring the Fracture Toughness of Mouse Bone.
      A.J. Makowski, S. Uppuganti, B. Rowland, A. Merkel, D.S. Perrien, J.A. Sterling, and **J.S. Nyman**. TGF-β Suppression with a Neutralizing Antibody Increases Vertebral Body Strength in Female Mice.
- Two publications related to the objective of the grant and published during the funding period
    - **J.S. Nyman** and A.J. Makowski. The Contribution of the Extracellular Matrix to the Fracture Resistance of Bone. *Current Osteoporosis Reports*. 10:169-77, 2012.
    - Lian, N., Lin, T., Liu, W., Wang, W., Li, L., Sun, S., **Nyman, J.S**. and X. Yang. Transforming Growth Factor β suppresses osteoblast differentiation via vimentin activating transcription factor 4 (ATF4) axis. *The Journal of Biological Chemistry*. 287:35975-84, 2012.
- Funding applied for based on work supported by this award
    - Assessing Bone Fracture Resistance with Reference Point Indentation. Vanderbilt's Institute for Clinical and Translational Research Grant. Objective: The objective is to determine if a local

measurement of bone quality by reference point indentation at a distal site is predictive of fracture resistance at a site that is prone to osteoporotic fracture.
    - Role of Vascularity and Matrix in Bone Brittleness. Vanderbilt Orthopaedic Institute Pilot Grant. Objective: The objectives are to determine whether a difference in blood vessel volume within bone decreases with aging in rodents and to identify matrix factors that potentially explain the loss of bone toughness with the loss of MMP-9 and aging.
- This award provided training experience for a graduate student (Alexander J. Makowski) pursuing a Ph.D.

CONCLUSION:

The inhibition of TGF-β by a commercially available antibody can improve the fracture resistance of cortical bone from aged animals. This is important because aging lowers fracture resistance beyond age-related loss in bone mass. The effect of TGF-β inhibition by antibody treatment is however complex as there were treatment differences in fracture resistance among different age groups of rodents. For example, 1D11 increased whole bone strength through an increase in structure when tested in old rats, but it only increased material strength (independent of structure) when tested in young growing mice. With the presented results, there is impetus to assess matrix proteins in order to identify the target of TGF-β that affects the resistance to crack propagation with advanced age.

REFERENCES:

[1] Kanis JA, Johnell O, Oden A, Dawson A, De Laet C, Jonsson B. Ten year probabilities of osteoporotic fractures according to BMD and diagnostic thresholds. Osteoporos Int 2001;12:989–995.

[2] Hui SL, Slemenda CW, Johnston CC. Age and bone mass as predictors of fracture in a prospective study. J. Clin. Invest. 1988;81:1804–1809.

[3] Ott SM. When bone mass fails to predict bone failure. Calcif Tissue Int 1993;53 Suppl 1:S7–13.

[4] Balooch G, Balooch M, Nalla RK, Schilling S, Filvaroff EH, Marshall GW, et al. TGF-beta regulates the mechanical properties and composition of bone matrix. Proc Natl Acad Sci USA 2005;102:18813–18818.

[5] Edwards JR, Nyman JS, Lwin ST, Moore MM, Esparza J, O'quinn EC, et al. Inhibition of TGF-β signaling by 1D11 antibody treatment increases bone mass and quality *in vivo*. J Bone Miner Res 2010;25:2419–2426.

[6] Keaveny TM, McClung MR, Wan X, Kopperdahl DL, Mitlak BH, Krohn K. Femoral strength in osteoporotic women treated with teriparatide or alendronate. Bone 2012;50:165–170.

[7] Pistoia W, van Rietbergen B, Lochmüller E-M, Lill CA, Eckstein F, Rüegsegger P. Estimation of distal radius failure load with micro-finite element analysis models based on three-dimensional peripheral quantitative computed tomography images. Bone 2002;30:842–848.

[8] Nyman JS, Lynch CC, Perrien DS, Thiolloy S, O'quinn EC, Patil CA, et al. Differential effects between the loss of MMP-2 and MMP-9 on structural and tissue-level properties of bone. J Bone Miner Res 2011;26:1252–1260.

[9] Silva MJ, Brodt MD, Lynch MA, McKenzie JA, Tanouye KM, Nyman JS, et al. Type 1 diabetes in young rats leads to progressive trabecular bone loss, cessation of cortical bone growth, and diminished whole bone strength and fatigue life. J Bone Miner Res 2009;24:1618–1627.

[10] Biswas S, Nyman JS, Alvarez J, Chakrabarti A, Ayres A, Sterling J, et al. Anti-transforming growth factor ß antibody treatment rescues bone loss and prevents breast cancer metastasis to bone. PLoS ONE 2011;6:e27090.

[11] Jepsen KJ, Akkus OJ, Majeska RJ, Nadeau JH. Hierarchical relationship between bone traits and mechanical properties in inbred mice. Mamm. Genome 2003;14:97–104.

APPENDICES:

Appendix A: ORS Abstract. Strength of Mouse Vertebral Bodies with μCT-derived Finite Element Analysis. Pages 9-12.

Appendix B: ASBMR Abstract. Measuring the Fracture Toughness of Mouse Bone. Pages 13-14.
Appendix C: ASBMR Abstract. TGF-β Suppression with a Neutralizing Antibody Increases Vertebral Body Strength in Female Mice. Pages 15-16.
Appendix D: Journal Article. The Contribution of the Extracellular Matrix to the Fracture Resistance of Bone. Pages 17-27.
Appendix E: Journal Article. Transforming Growth Factor β suppresses osteoblast differentiation via vimentin activating transcription factor 4 (ATF4) axis. Pages 28-37.

SUPPORTING DATA:

N/A because data figures and table are embedded in the report.

Print

Your abstract appears below.

Please print a copy of this page for your records.

To return to the Submission Center and check your list of submissions; click "View Submissions" in the left menu.

Proof

CONTROL ID: 1430915

TITLE: Assessing the Strength of Mouse Vertebral Bodies with µCT-derived Finite Element Analysis

AUTHORS (LAST NAME, FIRST NAME): Nyman, Jeffry S.[1, 2, 3]; Makowski, Alexander J.[2, 3]; Uppuganti, Sasidhar[1]; Sterling, Julie A.[3]; Perrien, Daniel S.[1]

INSTITUTIONS (ALL): 1. Department of Orthopaedics & Rehabilitation, Vanderbilt University, Nashville, TN, United States.
2. Department of Biomedical Engineering, Vanderbilt University, Nashville, TN, United States.
3. Department of Veterans Affairs, Tennessee Valley Healthcare System, Nashville, TN, United States.

CURRENT PRIMARY CATEGORY: Bone - Mechanics and Finite Element Analysis

AWARDS:

KEYWORDS: Bone Mechanics, Finite Element Analysis, Osteoporosis.

ABSTRACT BODY:

Introduction: Finite element analysis (FEA) can assess the strength of bone because quantitative computed tomography (qCT) scans can be converted to finite element (FE) models. The usefulness of qCT-FEA is evident in the growing number of clinical studies reporting that strength predictions derived from CT scans of hip, spine, or radius can differentiate fracture patients from non-fracture patients, though some overlap exists across the cohorts [1-2]. Much of the validation behind the failure criteria in these FE model predictions came from correlations with strength measurements as determined by whole bone testing of cadaveric tissue for which empirical relationships exist to convert mineral density to material properties. Given the relatively small size of mouse bones, especially vertebral bodies (VBs), no such relationships exist even though µCT-FEA could also be useful in pre-clinical and genetic studies involving mice. Since there is a dearth of evidence establishing the ability of µCT-FEA to assess mouse VB strength, we performed a parametric analysis to determine whether an elastic µCT-FEA with simple failure criteria could reasonably predict VB strength as

determined by compression tests.

Methods: Study design: We assessed the strength of VBs from 2 studies in which differences in BV/TV were expected from prior work: a TGFβ-neutralizing Ab (1D11) for 4 weeks increased trabecular bone volume fraction (BV/TV) [3] and mice lacking activating transcription factor 4 (ATF4) have a low BV/TV compared to wild-type mice [4]. Therefore, we treated 13-wk, male mice (FVB strain) with a control antibody (13C4, n=7) or 1D11 (n=8) for 4 weeks at the same dose (10 mg/kg 3x per wk). We aged Atf4+/+ (n=10) and Atf4-/- (n=10) mice (male and female on a FVB background) to 17 weeks. After euthanasia, L6 VBs were harvested and stored frozen in PBS.
μCT-FEA: All VBs were scanned at 12 μm voxel size using the same settings (μCT40, Scanco Medical) and hydroxyapatite (HA) phantom calibration. To calculate BV/TV, contours were manually drawn for the region between the end plates (Fig. 1), whereas to generate the FE model, a circle with a constant radius was copied into each image and positioned to transect the transverse processes, which do not bear load in the compression test (Fig. 2). For the VBs of the 1D11 study, a threshold of 421.4 mgHA/cm3 segmented bone from soft tissue and air. Then, using Scanco FEA elastic solver software (brick elements), the equivalent strains were determined for high-friction, axial compression loading of each VB at 1% apparent strain, elastic modulus (E) of 10 GPa, and υ of 0.03 for all elements. The reaction force was determined for initial failure criteria in which 2% of the model volume exceeds 0.7% equivalent strain (Base Model), which were the criteria in a validation study for human bone [5].
Parametric study: Keeping the failure criteria of the Base Model constant, the elastic modulus was increased to 18 GPa and 22 GPa. Next, E was held constant while varying the percentage of volume that must exceed 0.7% strain before failure. Instead of having one value for E across all VBs, modulus was also based on the tissue mineral density (TMD) of each VB using a conversion derived by Wagner et al. [7]. As one final change, we investigated the effect of increasing the threshold to 538.9 mgHA/cm3 (Fig. 2).
To verify applicability across studies, the strength of VBs from the ATF4 study were determined for a threshold of 450.8 mgHA/cm3, 18 GPa, 0.7% failure strain, and a critical volume of 2%.
Compression tests: Each hydrated VB was subjected to axial compression at 3 mm/min in which the supporting platen had a rough surface and a moment relief to minimize slippage and off-axis loading. Two VBs were removed due to translation.
Statistical analysis: The ability of μCT-FEA to predict mouse VB strength was ascertained by linear regression and the root mean squared error (RMSE).

Results: The Base Model FEA was not effective in predicting mouse VB strength (Fig. 3a) as the RMSE was rather high and the 95% confidence interval (CI) of the slope was above 1. However, increasing E of bone tissue reduced the error and led to a CI of 0.67 to 2.09, while not affecting the R^2 (Fig. 3b,c). Using an E based on mean TMD for each VB increased the ability of FEA to predict experimental strength (Fig. 3d). Varying the failure volume from 1% to 4% had modest effects on R^2 and RMSE: 1% (66.9% and 5.8), 2% (62.3% and 5.0), 3% (62.0% and 5.5), and 4% (61.9% and 6.3). Interestingly, whether using a constant E or VB-specific E, increasing the threshold to reduce the number of bony elements in the model improved the R^2 to 70.7% and 73.1%, respectively (Fig. 3b,e). Building confidence in this approach to μCT-FEA, the predicted strength also strongly correlated with experimental strength of the VBs from the Genetic study with low error (Fig. 3f). Even though the FE model includes the thin cortex, the ability of FEA to explain the variance in experimental strength was similar to that of trabecular BV/TV (1D11: R2 = 62.4% & Genetic: R2 = 83.6%).

Discussion: A μCT-derived elastic FEA can reasonably assess the strength of mouse VBs when the model has uniform isotropic material properties typical of bone (18 GPa) and uses simple failure criteria (2% of volume exceeds 0.7% equivalent strain). The choice of the threshold does influence the ability of μCT-FEA to predict VB strength, and as such, segmented images should be viewed for multiple VB scans across experimental groups. Using an E based on TMD can improve the prediction. Whether further improvements are gained with an inhomogeneous distribution of E and non-linear material behavior are yet to be determined. Compression tests of mouse VBs are prone to error owing to their small size and irregular shape.

As such, μCT-FEA is an attractive way to assess experimental effects on VB strength, especially if histology is desired. However, the predicted strengths should be interpreted in the context of the FEA assumptions, namely material behavior. If differences are expected at the material level, then compression tests should be carefully conducted.

Significance: This study provides evidence that μCT-FEA can predict mouse vertebral strength in pre-clinical studies assessing anti-fracture efficacy.

Acknowledgements: CDMRP Concept Award provided support.

References: [1] Orwoll et al. J Bone Miner Res 2009 [2] Vilayphiou et al. J Bone Miner Res 2011 [3] Edwards et al. J Bone Miner Res 2010 [4] Yang et al. Cell 2004 [5] Pistoia et al. Bone 2002 [6] Wagner et al. Bone 2011.

(No Table Selected)

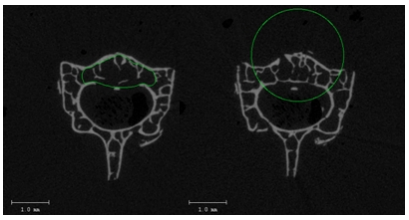

Figure 1. Hand contour for measuring BV/TV (left). Circle contour to generate finite model of the VB excluding the transverse processes.

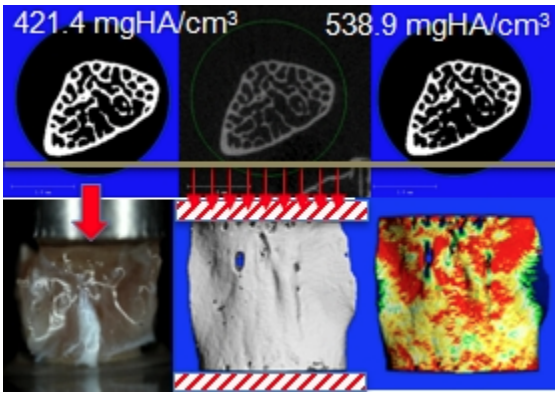

Figure 2. Segmentation of the μCT scans at 2 threshold values (above line). Compression test of the L6 vertebra, boundary conditions of the FE model of the VB, and equivalent strain distribution for compression (below line).

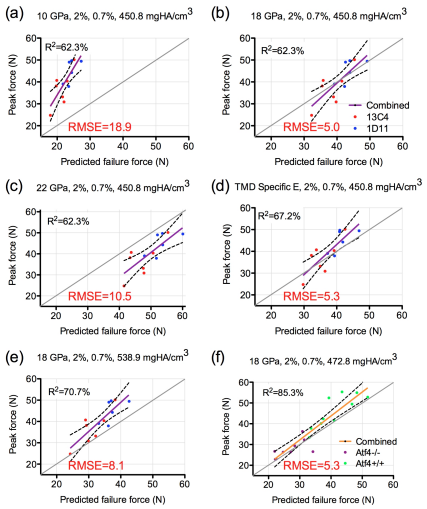

Figure 3. Linear regression with 95% confidence intervals for selected failure criteria and modulus assumptions (modulus of model, critical volume, failure strain, and threshold value is given in the title of each graph).

ASBMR 2012 Annual Meeting

Measuring the Fracture Toughness of Mouse Bone

Categories:
Bone Biomechanics and Quality (Basic)
Osteoporosis - Assessment
Poster Sessions, Presentation Number: SA0059
Session: Poster Session I and Poster Tours
Saturday, October 13, 2012 11:00 AM - 1:00 PM, Minneapolis Convention Center, Discovery Hall-Hall B

* Alexander Makowski, Department of Veterans Affairs Vanderbilt University, USA, Sasidhar Uppuganti, Vanderbilt University, USA, Jeffry Nyman, Vanderbilt University Medical Center, USA

The age-related increase in fracture risk may not be solely due to a loss in bone strength since bone matrix undergoes multiple changes independent of bone mineral density with aging and disease onset. To identify novel factors contributing to bone fracture resistance, a method was refined to quantify fracture toughness of rodent bone. This method involves generating a micro-notch in the cortex of the femur mid-shaft and loading the bone in three point bending to drive a crack from the notch through the matrix to failure. Quantifying this resistance to crack propagation as a material property known as the stress intensity factor (K_c) requires that the bone structure and the notch size be properly incorporated in the measurement. Given that the equations to do so were derived for a circular pipe and that the geometry of the mid-shaft is irregular varying across genotypes and strains, we investigated whether micro-notching the anterior vs. posterior side affects K_c using mouse strains with varying bone geometry. Femurs were harvested from nineteen 17 wk old male mice (FVB). To increase the variance in bone structure, femurs were also harvested from sixteen 11-12 wk old male, transgenic mice (on a mixed background), namely liver-specific insulin receptor knock-out (LIRKO) and cre-negative floxed mice (WT). Using a thin wafer saw and then a razor blade with µ-diamond solution, we obtained 15 anterior and 19 posterior notched bones meeting the geometry criteria. Notch angles and bone geometry were quantified from µCT scans acquired at 6 µm voxel size. Femurs were loaded at a rate of 0.06 mm/min to determine peak force and video was recorded (~14μm^2/pixel; 30 fps) to track failure mode. The COV of the notch angle was lower for the posterior than for the anterior group (12.4% vs. 21.1%). Video and µCT identified 2 specimens with deep notches and little cracking and 1 specimen with a partial notch and poor orientation. For the FVB mice, K_c is different between ant. and post. notched bones (Fig. 1). Also, K_c for post. notches differed between older FVB and younger LIRKO. Therefore, regressions to analyze independence of geometry were done separately (Fig. 1). For the ant. group, the y-intercept was not zero (95% CI: -3.97 to -0.93) suggesting a lack of independence. For the post. groups, this was not the case (FVB+WT 95% CI: -10.1 to 3.54). Further refinement of structure and notch angle analyses may help K_c become entirely independent of geometry.

Disclosures: J. Nyman, NSF: Research Grants.

*** Presenting Authors(s):** Alexander Makowski, Department of Veterans Affairs Vanderbilt University, USA

ATTACHMENTS

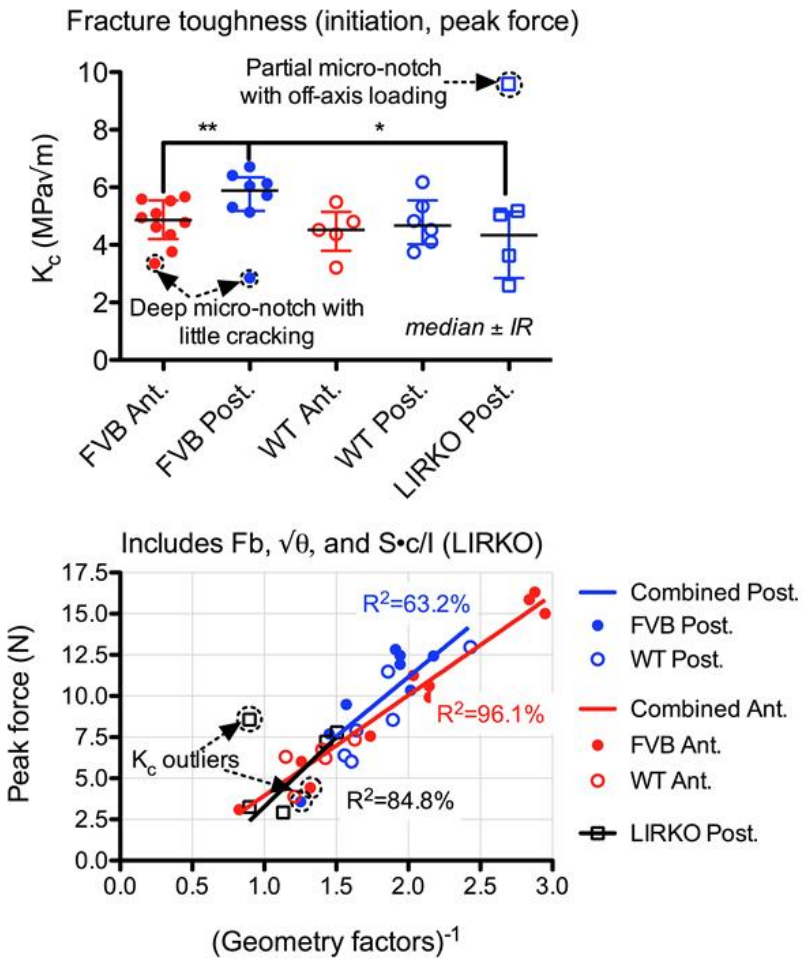

Fig 1. Fracture toughness for each group and regressions between geometry factors and peak force

Phone: +1 (202) 367-1161 Fax: +1 (202) 367-2161 Email: asbmr@asbmr.org
2025 M Street, NW, Suite 800 Washington, DC 20036-3309, USA

Follow Us:

ASBMR 2012 Annual Meeting

TGF-β Suppression with a Neutralizing Antibody Increases Vertebral Body Strength in Female Mice

Categories:
Osteoporosis - Treatment (Preclinical)
Bone Biomechanics and Quality (Basic)
Osteoporosis - Assessment
Poster Sessions, Presentation Number: SU0069
Session: Poster Session II and Poster Tours
Sunday, October 14, 2012 11:30 AM - 1:30 PM, Minneapolis Convention Center, Discovery Hall-Hall B

* Alexander Makowski, Department of Veterans Affairs Vanderbilt University, USA, Sasidhar Uppuganti, Vanderbilt University, USA, Barbara Rowland, Vanderbilt University, USA, Alyssa Merkel, Vanderbilt University, USA, Daniel Perrien, Vanderbilt University Medical Center, USA, Julie Sterling, Department of Veterans Affairs (TVHS)/Vanderbilt University Medical Center, USA, Jeffry Nyman, Vanderbilt University Medical Center, USA

Transforming growth factor beta (TGF-β) is a promising target for reversing the breast cancer-induced decrease in bone's resistance to fracture. Our previous work with a neutralizing antibody to the 3 isoforms of TGF-β (1D11) found that TGF-β suppression increased trabecular bone (BV/TV) in the long bones of both young female, tumor-bearing and older male, non-tumor bearing mice with an initial low bone mass phenotype (C57BL/6). To date, TGF-β suppression has only been reported to increase lumbar vertebra (VB) strength when young male (4 wk), non-tumor bearing mice are treated with an inhibitor of the TGF-β type I receptor kinase for 6 weeks. To test the hypothesis that 1D11 could be effective in enhancing fracture resistance in female mice, we treated 13 wk old FVB mice for 4 weeks with either 13C4 (control antibody, n=5) or 1D11 (10 mg/kg, n=7) 3x per week. After euthanasia, the L6 VB was scanned at an isotropic voxel size of 12 μm with a μCT scanner calibrated to a hydroxyapatite phantom. Using the scanner's finite element (FE) model generator (voxel-to-brick element) and elastic solver, the failure load of each VB was predicted for high-friction, axial compression at 1% apparent strain and using failure criteria in which 2% of the model volume exceeds 0.007 equivalent strain. We selected 2 cases of material properties (v = 0.03): constant modulus (CM) of 18 GPa and VB-specific modulus (SpM) derived from the mean tissue mineral density (TMD). Lastly, each VB was subjected to axial compression at 3 mm/min in which the supporting platen had a rough surface and a moment relief to minimize slippage and off-axis loading, respectively. The strength was the peak force sustained by the VB. Mann-Whitney was used to test for differences between groups. Compared to control, 1D11-treatment increased BV/TV by 41% and TMD by 3% (p=0.0025 for both) as well as increased the measured and predicted strengths (Fig. 1). After excluding an outlier (Fig. 1) that slipped during the compression test as observed by high magnification video, linear regression analysis found that BV/TV explained 75.8% of the variance in VB strength. Even though the μCT-FE analysis includes the cortical shell and trabecular architecture of the VB, the CM- and SpM-predicted strength explained 63.9% and 65.6%, respectively. Thus, TGF-β suppression apparently increases VB strength by increasing BV/TV with some contribution from an increase in TMD.

Disclosures: J. Sterling, VA: Research Grants. J. Nyman, VA: Research Grants.

*** Presenting Authors(s):** Alexander Makowski, Department of Veterans Affairs Vanderbilt University, USA

ATTACHMENTS

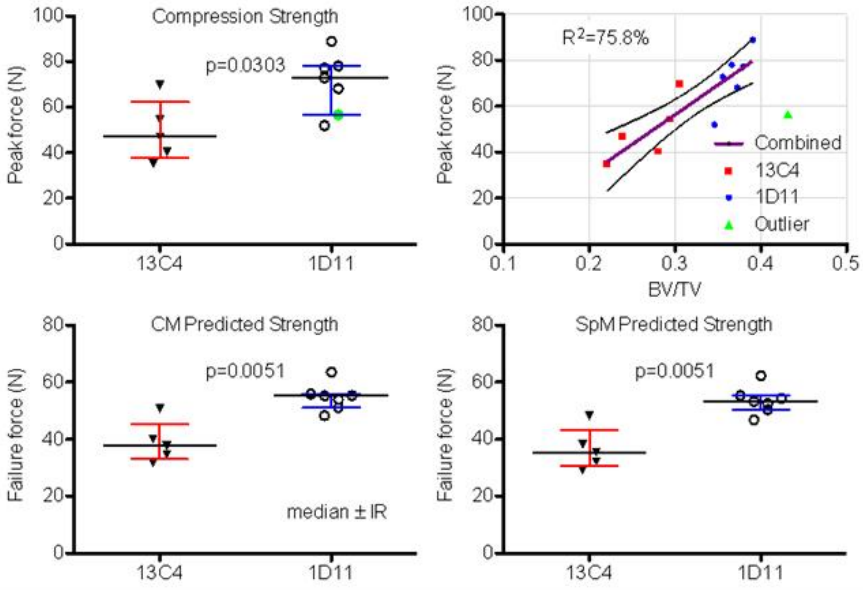

Figure 1. Vertebral body strength was greater for the 1D11-treated mice than control mice.

Phone: +1 (202) 367-1161 Fax: +1 (202) 367-2161 Email: asbmr@asbmr.org
2025 M Street, NW, Suite 800 Washington, DC 20036-3309, USA

Follow Us:

The Contribution of the Extracellular Matrix to the Fracture Resistance of Bone

Jeffry S. Nyman & Alexander J. Makowski

Current Osteoporosis Reports

ISSN 1544-1873

Curr Osteoporos Rep
DOI 10.1007/s11914-012-0101-8

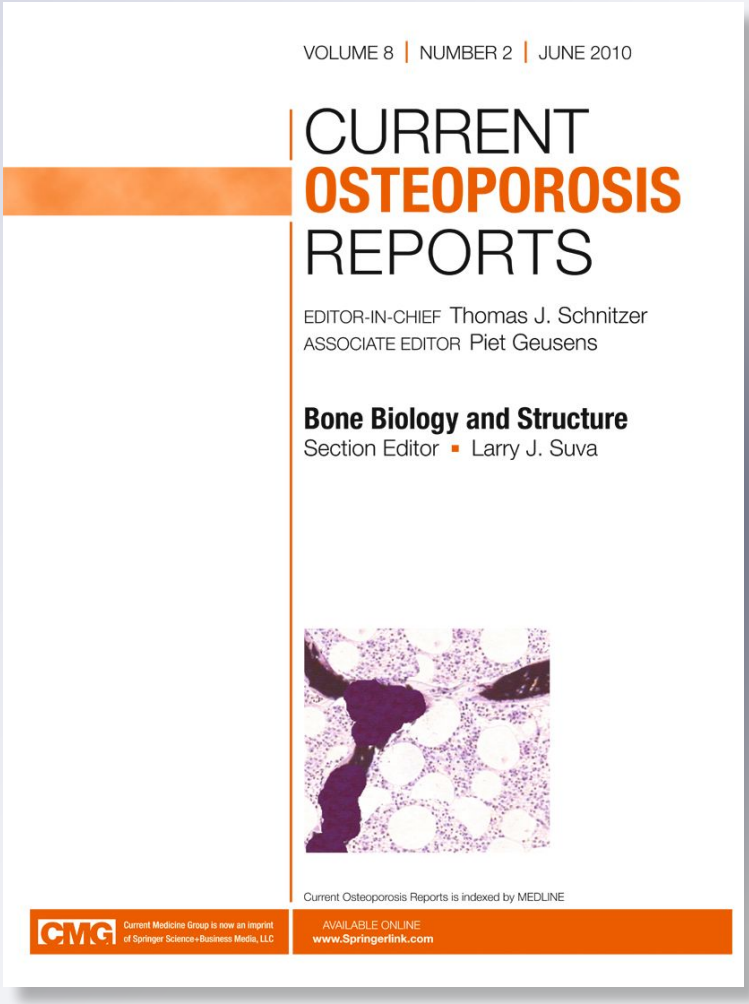

Springer

Curr Osteoporos Rep
DOI 10.1007/s11914-012-0101-8

SKELETAL REGULATIONS (D GADDY, SECTION EDITOR)

The Contribution of the Extracellular Matrix to the Fracture Resistance of Bone

Jeffry S. Nyman · Alexander J. Makowski

Abstract The likelihood of suffering a bone fracture is not solely predicated on areal bone mineral density. As people age, there are numerous changes to the skeleton occurring at multiple length scales (from millimeters to submicron scales) that reduce the ability of bone to resist fracture. Herein is a review of the current knowledge about the role of the extracellular matrix (ECM) in this resistance, with emphasis on engineering principles that characterize fracture resistance beyond bone strength to include bone toughness and fracture toughness. These measurements of the capacity to dissipate energy and to resist crack propagation during failure precipitously decline with age. An age-related loss in collagen integrity is strongly associated with decreases in these mechanical properties. One potential cause for this deleterious change in the ECM is an increase in advanced glycation end products, which accumulate with aging through nonenzymatic collagen crosslinking. Potential regulators and diagnostic tools of the ECM with respect to fracture resistance are also discussed.

Keywords Bone quality · Toughness · Strength · Fracture toughness · Collagen · Structure · Architecture · Microdamage · Porosity · Biomechanics · Fracture risk · AGEs · Osteoporosis · Diabetes · Aging · Finite element analysis · Noncollagenous proteins · Mineral · TGF-β · Crosslinking · Matrix metalloproteinase

Introduction

The risk of suffering a bone fracture increases with age, and in addition to postmenopausal osteoporosis, certain diseases such as diabetes [1] and chronic kidney disease [2] also increase fracture risk. While an age-related or diabetes-related propensity to fall can certainly increase the chance of breaking a bone [3], the skeleton does undergo deleterious changes with aging and disease onset, and these changes reduce the ability of bone to resist fracture. One well-recognized change is a loss of bone mass, and as such, osteoporosis therapies are designed to prevent bone loss (eg, bisphosphonates [BisPs]) or promote bone gain (eg, intermittent parathyroid hormone). Moreover, assessment of bone loss as a T-score or Z-score derived from dual-energy X-ray absorptiometry (DXA) is used clinically to assess fracture risk.

Despite the effectiveness of antiresorptive therapy [4] and bone anabolic therapy [5] in increasing DXA-derived areal bone mineral density (aBMD) and more importantly reducing the incidence of fracture, certain individuals still sustain fractures with treatment. In addition, long-term BisP use has been associated with atypical, subtrochanteric fractures, although

J. S. Nyman · A. J. Makowski
Department of Veterans Affairs,
Tennessee Valley Healthcare System,
Nashville, TN 27212, USA
e-mail: a.makowski@vanderbilt.edu

J. S. Nyman
Department of Orthopaedics & Rehabilitation,
Vanderbilt University,
Nashville, TN 37232, USA

J. S. Nyman · A. J. Makowski
Vanderbilt Center for Bone Biology, Vanderbilt University,
Nashville, TN 37232, USA

J. S. Nyman · A. J. Makowski
Department of Biomedical Engineering, Vanderbilt University,
Nashville, TN 37232, USA

J. S. Nyman (✉)
Vanderbilt Orthopaedic Institute, Medical Center East,
South Tower, Suite 4200,
Nashville, TN 37232, USA
e-mail: jeffry.s.nyman@vanderbilt.edu

Published online: 13 April 2012

no causal link has been established to date [6]. Thus, fractures are not solely the result of low bone mass or density, and treatment-related reductions in fracture incidence are not solely explained by changes in aBMD [7].

As further evidence supporting the notion that bone mass is not the sole determinant of fracture resistance, aBMD is not a particularly accurate predictor of an individual's risk of fracture, with many fractures occurring in subjects with T-scores below −2.5 (the number of standard deviation below or above young adult normal mean aBMD) [8]. In effect, the age-related increase in fracture risk is independent of the age-related decrease in BMD [8, 9]. That is, a 70-year-old is at a much greater risk of breaking a bone than a 50-year-old with the same BMD, an observation first published in the 1980s [10]. In addition to aging, the diabetes-associated increased risk of bone fracture is disproportionate to differences in aBMD between diabetic and age-matched nondiabetic patients [11]. Type 2 diabetes (T2DM) is not necessarily associated with lower BMD [12], and, in several studies, aBMD was actually found to be higher in T2DM patients [11, 13] than in age-matched, nondiabetic patients. This inability of aBMD to predict individual fracture risk has various origins, but one indication is that aging and certain diseases affect bone in ways that are invisible to DXA-derived measures of bone mass (eg, collagen integrity [14]). Capturing the importance of non-BMD factors, bone quality was defined in a National Institutes of Health conference as "the sum total of characteristics of the bone that influence the *bone's resistance to fracture*" [15]. Those characteristics span the multiple length scales, from millimeters to submicrons, comprising the hierarchical organization of bone and include the extracellular matrix (ECM).

Besides bone mass, cortical bone structure and trabecular bone architecture are determinants of fracture resistance. Avoiding the DXA limitations of acquiring measurements from a two-dimensional projection, quantitative, X-ray computed tomography (QCT) provides both structural parameters and volumetric BMD (in equivalent density of a hydroxyapatite phantom). High-resolution peripheral CT (HR-pQCT) can provide additional architectural parameters such as trabecular thickness and connectivity density [16]. With regard to cortical bone structure, moment of inertia and cross-sectional area correlate with whole-bone strength as determined by biomechanical testing of cadaveric femurs and radii in simulated fall configurations (Fig. 1) [17, 18]. In clinical studies involving QCT, patients with a femoral neck or trochanteric fracture had a smaller cortical cross-sectional area and lower moment of inertia at the neck than age-matched non-fracture patients [19], indicating decreased bone strength. The importance of bone structure to fracture resistance has been further demonstrated in recent studies that used the finite element method (FEM) to predict bone strength from patients' CT scan of the hip and found strength was strongly associated with fracture risk [20, 21••]. In addition, QCT-FEM assessment of vertebral body strength had a greater ability of discriminating vertebral fractures than areal BMD or volumetric BMD in a cross-sectional study of postmenopausal women [22]. Nonetheless, given that fractures can arise from fatigue loading, and that the fracture process involves the growth of cracks through the bone tissue, bone strength is not likely the sole contributor to a fracture event. Fracture resistance of bone also depends on the inherent quality of the ECM as described herein.

Age-Related Changes in Bone Toughness

From the 1960s to the present, studies involving the mechanical testing of fresh frozen, cadaveric bone have identified numerous age-related determinants of bone's resistance to fracture (Table 1). In these cadaveric studies, bone samples are milled or cored to produce specimens with uniform geometry at the length scale of several millimeters (Fig. 1) [23], which is 10–20 times greater than the size of an osteon or trabecula. With respect to cortical bone, aging affects the ability of bone to dissipate energy during failure (bone toughness) to a greater extent than it does the material strength [24–27]. Basically, older bone is brittle while younger bone is ductile, and this age-related change is primarily due to a loss in the ability of aged bone to deform or stretch beyond the point at which damage begins to form in the ECM (ie, yield point or proportional limit) [27]. The exact mechanism causing a decrease in bone toughness with age still requires further investigation. However, it is known that the organic phase of the ECM, namely type 1 collagen, is primarily responsible for bone toughness. For example, in mechanical testing studies of cadaveric bone, an age-related decrease in the stability of collagen correlated with bone toughness [26] as did an age-related decrease in collagen content [27]. In addition, manipulations to the collagen, such as thermal-induced collagen denaturation [28], formalin fixation [29], and high-energy, gamma or X-ray irradiation [30, 31], reduce the toughness of bone without necessarily affecting its material strength.

Fracture Toughness as a Measurement of Fracture Resistance

In engineering mechanics, strength is not the only material property guiding design. Since all materials have flaws or void spaces, however small, there is potential for a crack to form during the service life of the material. If the crack reaches a critical size, failure of the material is inevitable. Therefore, there are mechanical tests that characterize the ability of a material to resist crack initiation and crack propagation (a.k.a. fracture toughness) in addition to those that measure strength (yield or peak stress) and toughness (area

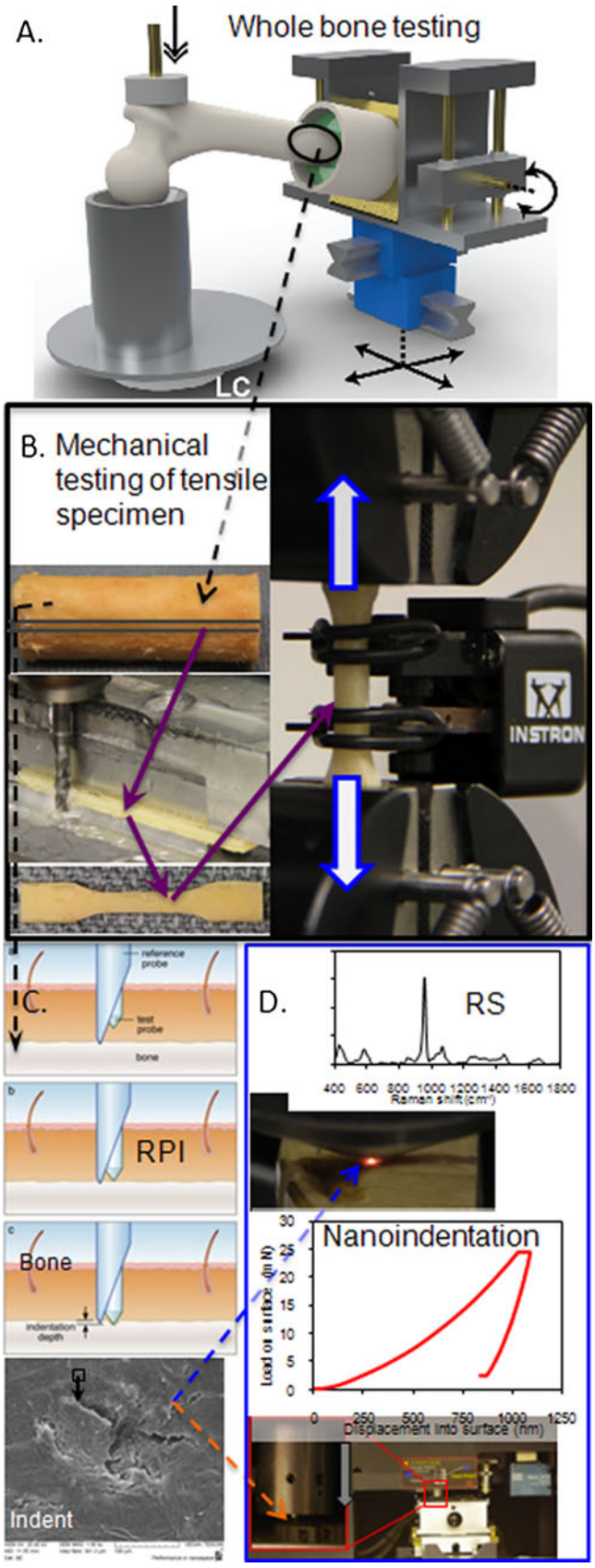

Fig. 1 To fully characterize the contributors to the fracture resistance of bone, the tissue is tested at multiple length scales, which involves analyses at progressively smaller length-scales: **a,** macrostructure (> 10 mm), testing of a femur in a sideways fall configuration to quantify whole-bone strength; **b,** submacrostructure (2–5 mm), tensile mechanical testing of uniform cortical bone strips to quantify apparent material propeties; **c,** microstructure (150–350 μm), reference point indentation (RPI) to characterize in situ or in vivo damage resistance of the extracellular matrix, as shown in the scanning electron micrograph in the *lower portion of the panel*; **d,** submicrostructure (0.5–25 μm), Raman spectroscopy (RS) to assess compositional properties of the matrix such as mineral-to-collagen ratio and crystallinity and nanoindentation to acquire complementary properties of modulus and hardness

under the stress-vs-strain cure). Whether measured by the critical stress intensity factor [32, 33] or the strain energy release rate [34, 35], fracture toughness of human bone decreases during aging (Table 1). Moreover, healthy bone tissue possesses the ability to demand greater energy to continue propagating a crack as the crack grows in length (ie, R-curve behavior) [36, 37], and this behavior is lost or reduced with aging [38, 39].

The determinants of fracture toughness are rather complex, spanning multiple length scales (Table 1), and as such, clinical surrogates of fracture toughness are not obvious. With respect to mechanism, Vashishth et al. [40, 41] observed the formation of microscopic cracks within the ECM of bone—bovine, antler, and human—occupying "process zones" ahead and in the wake of a propagating crack. Nalla et al. [42] and Zimmermann et al. [43•] further observed unbroken "ligaments" of bone tissue along the path of the propagating crack. As explained by Ritchie [44], these processes contribute to toughening, with an intrinsic mechanism of formation of the frontal microdamage zone and extrinsic mechanisms of crack bridging within the ECM as well as crack deflection around osteons. The exact changes in the ECM affecting these mechanisms remain to be fully elucidated, but age-related increases in nonenzymatic collagen crosslinking are implicated [43•, 45, 46].

The aforementioned observations of toughening mechanisms were made through analyses of ex vivo bone samples using nonclinical instruments such as scanning electron microscopy and synchrotron micro-CT (SR-μCT). Perhaps the closest clinical measurement of bone's resistance to crack propagation is the indentation distance increase (IDI) that is quantified using reference point indentation (RPI). Unlike microindentation or nanoindentation in which a hard tip (eg, diamond) penetrates the material such that depth, force, and contact area are recorded to quantify hardness and modulus, RPI utilizes a reference probe (akin to a hypodermic needle) and a test probe that slides through the reference probe indenting the bone tissue (Fig. 1) [47]. Moreover, RPI is designed for clinical use. Specifically, the RPI reference probe engages the patient's bone under the periosteum of the tibial mid-shaft; the test probe performs 20 cycles of microindents into the tissue (50–100 μm in diameter x 100–200 μm in depth) in force control; and then, among other properties, the instrument

Table 1 Age-related changes in bone at different length scales have been associated with changes in fracture resistance

Length scale, μm	Bone tissue characteristic	Material property	Reference
100	↑ Osteons per area	↓ Tensile strength	[23]
100	↑ Percentage osteons	↓ Resistance to crack propagation	[34]
10–50	↑ Porosity	↓ Post-yield toughness	[25]
10–50	↑ Porosity	↓ Resistance to crack propagation	[35]
1–5	↑ Microdamage	↓ Resistance to crack propagation	[33]
0.1	↓ Collagen integrity	↓ Toughness	[26]
0.1	↑ Collagen crosslinks	↓ Fracture toughness	[45]
0.1	↓ Collagen content	↓ Post-yield energy dissipation	[27]

records IDI, the relative distance that the test probe travels into the ECM of bone. During indentation, microdamage forms below the indenter (Fig. 1), and presumably, bone matrix with less resistance to microdamage formation allows the test probe to penetrate deeper than bone matrix with high resistance. Recently, the IDI for 27 fracture patients was observed to be 47% greater than the IDI for 8 age-matched patients (P= 0.008) in the same hospital for non-fracture reasons [48••]. Using cadaveric bone from several donors, IDI was found to be inversely proportional to crack growth toughness [48••], thus linking local indents to apparent-level fracture toughness.

Formation of Fatigue Microdamage in the Extracellular Matrix

Although the bone's ECM dissipates energy through the generation of microdamage as a means to improve its fracture toughness, bone must still minimize the accumulation of fatigue-induced microdamage in non-cracked regions. When subjected to repeated (ie, cyclic) loading over time at stresses well below the yield strength of bone, the bone matrix accumulates linear microcracks and diffuse patches of nanocracks. Among other functions, bone remodeling serves to remove this fatigue-induced microdamage [49, 50]. Nonetheless, the degree of microdamage in bone increases with age [51, 52], suggesting age-related changes in bone's ECM favors microdamage formation. Certainly, engineering measurements of fatigue properties such as fatigue life (number of cycles to failure, N_f) and fatigue strength (y-intercept on an applied stress vs N_f semi-log curve) of cadaveric bone decrease with age [53, 54]. The changes in the ECM that lead to such declines are not fully understood, but fatigue microdamage is known to accumulate between osteons in the interstitial sites [55], and interstitial sites (ie, remnants of remodeled osteons) have an older tissue age with higher mineral-to-collagen ratio [56] and greater concentrations of mature collagen crosslinks [57]. Moreover, the number of lacunae in the ECM and the degree of mineralization in peri-lacunar space has been observed to decrease and increase, respectively, with age [58•]. Also, greater microdamage has been associated with a reduction in osteocyte lacunar density [59]. Thus, a "brittling" of the ECM with human and tissue age lowers the tissue strain surrounding a crack, allowing it to propagate through microstructural barriers like cement lines, as recently observed for human cortical bone [60].

Organic Contribution to Fracture Resistance: Collagen, AGEs, and NCPs

As previously discussed, type 1 collagen, which comprises 90% of the organic matrix, is the primary determinant of bone toughness. It is critical to overall fracture resistance, even though increasing mineral content is still the primary focus of drug discovery for fracture prevention. The classic example of collagen's importance in bone is osteogenesis imperfecta (OI), known as the brittle bone disease, in which mutations in the gene encoding collagen strands (*col1a1*) lead to various grades of severity in the loss of fracture resistance. OI mice have bones with less post-yield deformation (ie, more brittle) than do wild-type mice [61, 62], and there is greater microdamage formation with altered morphology in OI bones [63]. Beyond this defect in collagen that causes other changes in the matrix (eg, crystallinity), crosslinking is also important. For example, disrupting enzymatic collagen crosslinking by treating rats with a lysyl oxidase inhibitor reduces bone strength without affecting mineralization [64].

Increases in advanced glycation end products (AGEs) perhaps have garnered the greatest attention as a potential change in the organic matrix causing a decrease in fracture resistance of bone. Formed through a nonenzymatic reaction process involving sugar, these crosslinks of collagen increase in concentration with age and diabetes, even though bone turns over or remodels. Age-related increases in pentosidine, a quantifiable biomarker of AGEs, are associated with a decrease in post-yield energy dissipation and fracture toughness of bone [27, 45]. Clinically, serum or urine levels of pentosidine have been associated with higher incidence of fracture in postmenopausal women [65, 66••] and subjects with T2DM [67, 68]. The concentration of pentosidine is higher in rodents with diabetes relative to control bone [69], and given enough time

for diabetes to progress in rodents, bones become brittle [70]. Although a mechanism is not fully delineated, one possibility is that AGEs stiffen the collagen matrix such that the fibrils dissipate less energy, allowing microdamage to more readily form and propagate through the ECM.

Recently, attention has also been given to noncollagenous proteins (NCPs) as contributors to the fracture resistance of bone. Initially, small-scale mechanics using atomic force microscopy demonstrated that phosphorylated proteins can bridge neighboring mineralized collagen fibrils forming so-called sacrificial bonds resisting fibril separation [71]. Subsequently, osteopontin (OPN) was one NCP observed to dissipate energy through this mechanism [72]. Mice lacking osteopontin (OPN−/− mice) have bones with 30% lower fracture toughness compared to wild-type bones. However, it should be noted that this difference may not solely be due to the role of OPN as a sacrificial bonding agent since OPN is involved in mineralization and OPN−/− bones exhibited greater tissue heterogeneity than OPN+/+ bones [73]. Interestingly, osteonal tissue has higher amounts of OPN and osteocalcin than does interstitial tissue [74], and as previously mentioned, interstitial sites are where microcracks are most often observed in cortical bone.

The Role of Water in Fracture Resistance

As an essential component of the ECM, water is bound to both collagen and mineral phases via hydrogen-hydrogen bonding. As the amount of water removal from human cortical bone increases with an increase in drying temperature (24°C to 50°C to 70°C), the toughness of bone significantly decreases, suggesting loosely and tightly bound water contribute to fracture resistance [75]. Using solid-state nuclear magnetic resonance (NMR), a structural layer of water was observed between the collagen and mineral phases of bone [76] and could act as another sacrificial layer protecting collagen fibrils from shear forces [76]. Measurements of bound water using ^{1}H NMR spectroscopy have been correlated with the mechanical properties of human cortical bone [77, 78], and if successfully translated to clinical imaging (magnetic resonance imaging), bound water could potentially be an important indicator of fracture resistance.

Spectroscopic Characterization of Bone Tissue with Respect to Fracture Resistance

Fourier transform infrared (FTIR) and Raman spectroscopy (RS) are two complementary optical techniques widely used to gain insight into the biophysical nature of bone's ECM as it relates to fracture resistance. In brief, when light impinges on chemical bonds, energy is gained or lost depending on the light wavelength and molecular vibrations of the chemical moieties in the tissue. The intensity spectrum of collected light (Fig. 1) corresponds to the biochemical distribution of the bone matrix. FTIR indirectly measures differential absorption of light by anti-symmetric vibrations through the attenuation of transmitted infrared wavelengths. Due to water absorption, FTIR usually requires thin, dehydrated ex vivo samples [79]. RS utilizes direct reflectance measures of differential scattering off symmetric vibrations, shifted relative to the input wavelength. Despite added complications from concurrent fluorescence, RS with its reflectance design has clinical potential as a noninvasive instrument for bone matrix measures in situ and even diagnostic capability through skin [80, 81].

While the potential for optical spectroscopy to assess fracture resistance clinically is nascent, many studies into the ECM of bone have already contributed to our understanding of fracture resistance. Investigations utilizing optical spectroscopies have demonstrated the following: FTIR sensitivity to many processes involved in matrix mineralization [82]; Raman sensitivity to damage and defects in the bone matrix [83]; and Raman spectral changes in the ECM related to age-related changes in the mechanical properties of cortical bone [84, 85]. Building upon established Raman markers of bone quality [86], we recently demonstrated consistent Raman measurements of compositional differences between osteonal and interstitial tissue from human cortical bone across bone orientation and processing conditions [56].

Recently, there have been efforts to determine whether spectroscopy can assess fracture risk and treatment-related changes to the ECM. Expanding upon evidence for a spectroscopic profile of osteoporosis [87], Boskey et al. [88] analyzed iliac crest biopsies with FTIR. They correlated matrix turnover rates of osteoporotic bone with relative tissue homogeneity and specifically demonstrated globally decreased mineral-to-matrix ratio and increased crystal size in tissue from patients with osteoporosis. In another FTIR study, Gourion-Arsiquaud et al. [89] showed that fragility fractures were associated with locally increased mineral content, carbonate substitution, and collagen crosslinking. Interestingly, carbonate substitution provided the greatest difference between fracture and non-fracture patients. Moreover, the associations of the FTIR-derived properties of mature-to-immature collagen crosslinking ratio and mineral-to-collagen ratio with fracture risk were independent of aBMD. Further insight into the effects of BisPs on bone matrix was provided by Gourion-Arsiquaud et al. [89]. They examined the tibia of beagles after 1 year of BisP treatment and found increased mineral content and increased collagen crosslinking maturity that was also more homogenous than bone from untreated controls [90]. Then, in an FTIR analysis of iliac crest samples obtained from patients enrolled in the Fracture Prevention Trial, Paschalis et al. [91] showed a spectral profile of teriparatide (recombinant human parathyroid hormone)-

Curr Osteoporos Rep
DOI 10.1007/s11914-012-0101-8

SKELETAL REGULATIONS (D GADDY, SECTION EDITOR)

The Contribution of the Extracellular Matrix to the Fracture Resistance of Bone

Jeffry S. Nyman · Alexander J. Makowski

Abstract The likelihood of suffering a bone fracture is not solely predicated on areal bone mineral density. As people age, there are numerous changes to the skeleton occurring at multiple length scales (from millimeters to submicron scales) that reduce the ability of bone to resist fracture. Herein is a review of the current knowledge about the role of the extracellular matrix (ECM) in this resistance, with emphasis on engineering principles that characterize fracture resistance beyond bone strength to include bone toughness and fracture toughness. These measurements of the capacity to dissipate energy and to resist crack propagation during failure precipitously decline with age. An age-related loss in collagen integrity is strongly associated with decreases in these mechanical properties. One potential cause for this deleterious change in the ECM is an increase in advanced glycation end products, which accumulate with aging through nonenzymatic collagen crosslinking. Potential regulators and diagnostic tools of the ECM with respect to fracture resistance are also discussed.

Keywords Bone quality · Toughness · Strength · Fracture toughness · Collagen · Structure · Architecture · Microdamage · Porosity · Biomechanics · Fracture risk · AGEs · Osteoporosis · Diabetes · Aging · Finite element analysis · Noncollagenous proteins · Mineral · TGF-β · Crosslinking · Matrix metalloproteinase

Introduction

The risk of suffering a bone fracture increases with age, and in addition to postmenopausal osteoporosis, certain diseases such as diabetes [1] and chronic kidney disease [2] also increase fracture risk. While an age-related or diabetes-related propensity to fall can certainly increase the chance of breaking a bone [3], the skeleton does undergo deleterious changes with aging and disease onset, and these changes reduce the ability of bone to resist fracture. One well-recognized change is a loss of bone mass, and as such, osteoporosis therapies are designed to prevent bone loss (eg, bisphosphonates [BisPs]) or promote bone gain (eg, intermittent parathyroid hormone). Moreover, assessment of bone loss as a T-score or Z-score derived from dual-energy X-ray absorptiometry (DXA) is used clinically to assess fracture risk.

Despite the effectiveness of antiresorptive therapy [4] and bone anabolic therapy [5] in increasing DXA-derived areal bone mineral density (aBMD) and more importantly reducing the incidence of fracture, certain individuals still sustain fractures with treatment. In addition, long-term BisP use has been associated with atypical, subtrochanteric fractures, although

J. S. Nyman · A. J. Makowski
Department of Veterans Affairs,
Tennessee Valley Healthcare System,
Nashville, TN 27212, USA
e-mail: a.makowski@vanderbilt.edu

J. S. Nyman
Department of Orthopaedics & Rehabilitation,
Vanderbilt University,
Nashville, TN 37232, USA

J. S. Nyman · A. J. Makowski
Vanderbilt Center for Bone Biology, Vanderbilt University,
Nashville, TN 37232, USA

J. S. Nyman · A. J. Makowski
Department of Biomedical Engineering, Vanderbilt University,
Nashville, TN 37232, USA

J. S. Nyman (✉)
Vanderbilt Orthopaedic Institute, Medical Center East,
South Tower, Suite 4200,
Nashville, TN 37232, USA
e-mail: jeffry.s.nyman@vanderbilt.edu

Published online: 13 April 2012

Disclosures Conflicts of interest: J.S. Nyman: has received grant support from National Science Foundation, Department of Defense, Veterans Affairs; and has a patent (planned, pending or issued) for Vanderbilt University and the Department of Veterans Affairs for U.S. Provisional Application No. 61/369,248: System and Method for Determining Mechanical Properties of Bone Structures; A.J. Makowski: none.

References

Papers of particular interest, published recently, have been highlighted as:

- • Of importance
- •• Of major importance

1. Janghorbani M, Van Dam RM, Willett WC, Hu FB. Systematic review of type 1 and type 2 diabetes mellitus and risk of fracture. Am J Epidemiol. 2007;166(5):495–505.
2. Nickolas TL, Leonard MB, Shane E. Chronic kidney disease and bone fracture: a growing concern. Kidney Int. 2008;74(6):721–31.
3. Stevens JA, Olson S. Reducing falls and resulting hip fractures among older women. Home Care Provider. 2000;5(4):134–9. quiz 140–131.
4. Watts NB. Treatment of osteoporosis with bisphosphonates. Rheum Dis Clin North Am. 2001;27(1):197–214.
5. Neer RM, Arnaud CD, Zanchetta JR, et al. Effect of parathyroid hormone (1–34) on fractures and bone mineral density in postmenopausal women with osteoporosis. N Engl J Med. 2001;344 (19):1434–41.
6. Shane E, Burr D, Ebeling PR, et al. Atypical subtrochanteric and diaphyseal femoral fractures: report of a task force of the American Society for Bone and Mineral Research. J Bone Miner Res. 2010;25 (11):2267–94.
7. Chen P, Miller PD, Delmas PD, et al. Change in lumbar spine BMD and vertebral fracture risk reduction in teriparatide-treated postmenopausal women with osteoporosis. J Bone Miner Res. 2006;21(11):1785–90.
8. Kanis JA, Johnell O, Oden A, et al. Ten year probabilities of osteoporotic fractures according to BMD and diagnostic thresholds. Osteoporos Int. 2001;12(12):989–95.
9. Siris ES, Brenneman SK, Barrett-Connor E, et al. The effect of age and bone mineral density on the absolute, excess, and relative risk of fracture in postmenopausal women aged 50–99: results from the National Osteoporosis Risk Assessment (NORA). Osteoporos Int. 2006;17(4):565–74.
10. Hui SL, Slemenda CW, Johnston Jr CC. Age and bone mass as predictors of fracture in a prospective study. J Clin Invest. 1988;81(6):1804–9.
11. de II L, van der Klift M, de Laet CE, et al. Bone mineral density and fracture risk in type-2 diabetes mellitus: the Rotterdam Study. Osteoporos Int. 2005;16(12):1713–20.
12. Hampson G, Evans C, Petitt RJ, et al. Bone mineral density, collagen type 1 alpha 1 genotypes and bone turnover in premenopausal women with diabetes mellitus. Diabetologia. 1998;41 (11):1314–20.
13. Vestergaard P. Discrepancies in bone mineral density and fracture risk in patients with type 1 and type 2 diabetes–a meta-analysis. Osteoporos Int. 2007;18(4):427–44.
14. Zioupos P. Ageing human bone: factors affecting its biomechanical properties and the role of collagen. J Biomater Appl. 2001;15 (3):187–229.
15. Fyhrie DP. Summary–Measuring "bone quality". J Musculoskelet Neuronal Interact. 2005;5(4):318–20.
16. Nickolas TL, Stein E, Cohen A, et al. Bone mass and microarchitecture in CKD patients with fracture. J Am Soc Nephrol. 2010;21(8):1371–80.
17. Cheng XG, Lowet G, Boonen S, et al. Assessment of the strength of proximal femur in vitro: relationship to femoral bone mineral density and femoral geometry. Bone. 1997;20(3):213–8.
18. Lochmuller EM, Lill CA, Kuhn V, et al. Radius bone strength in bending, compression, and falling and its correlation with clinical densitometry at multiple sites. J Bone Miner Res. 2002;17(9):1629–38.
19. Ito M, Wakao N, Hida T, et al. Analysis of hip geometry by clinical CT for the assessment of hip fracture risk in elderly Japanese women. Bone. 2010;46(2):453–7.
20. Orwoll ES, Marshall LM, Nielson CM, et al. Finite element analysis of the proximal femur and hip fracture risk in older men. J Bone Miner Res. 2009;24(3):475–83.
21. •• Amin S, Kopperdhal DL, Melton LJ, 3rd, et al.: Association of hip strength estimates by finite-element analysis with fractures in women and men. J Bone Miner Res 2011, 26(7): 1593–1600. *Accounting for the contribution of bone structure to hip strength, finite element analysis of computed tomgoraphy scans acquired from 580 subjects could predict osteoporotic fractures with a predicted strength of less than 3000 N being the critical threshold for skeletal fragility.*
22. Imai K, Ohnishi I, Matsumoto T, et al. Assessment of vertebral fracture risk and therapeutic effects of alendronate in postmenopausal women using a quantitative computed tomography-based nonlinear finite element method. Osteoporos Int. 2009;20 (5):801–10.
23. Evans FG. Mechanical properties and histology of cortical bone from younger and older men. Anat Rec. 1976;185(1):1–11.
24. Burstein AH, Reilly DT, Martens M. Aging of bone tissue: mechanical properties. J Bone Joint Surg Am. 1976;58(1):82–6.
25. McCalden RW, McGeough JA, Barker MB, Court-Brown CM. Age-related changes in the tensile properties of cortical bone. The relative importance of changes in porosity, mineralization, and microstructure. J Bone Joint Surg Am. 1993;75(8):1193–205.
26. Zioupos P, Currey JD, Hamer AJ. The role of collagen in the declining mechanical properties of aging human cortical bone. J Biomed Mater Res. 1999;45(2):108–16.
27. Nyman JS, Roy A, Tyler JH, et al. Age-related factors affecting the postyield energy dissipation of human cortical bone. J Orthop Res. 2007;25(5):646–55.
28. Wang X, Bank RA, TeKoppele JM, Agrawal CM. The role of collagen in determining bone mechanical properties. J Orthop Res. 2001;19(6):1021–6.
29. Stefan U, Michael B, Werner S. Effects of three different preservation methods on the mechanical properties of human and bovine cortical bone. Bone. 2010;47(6):1048–53.
30. Currey JD, Foreman J, Laketic I, et al. Effects of ionizing radiation on the mechanical properties of human bone. J Orthop Res. 1997;15(1):111–7.
31. Barth HD, Launey ME, Macdowell AA, et al. On the effect of X-ray irradiation on the deformation and fracture behavior of human cortical bone. Bone. 2010;46(6):1475–85.
32. Zioupos P, Currey JD. Changes in the stiffness, strength, and toughness of human cortical bone with age. Bone. 1998;22(1):57–66.
33. Zioupos P. Accumulation of in-vivo fatigue microdamage and its relation to biomechanical properties in ageing human cortical bone. JMicrosc. 2001;201(2):270–8.
34. Yeni YN, Brown CU, Wang Z, Norman TL. The influence of bone morphology on fracture toughness of the human femur and tibia. Bone. 1997;21(5):453–9.
35. Yeni YN, Brown CU, Norman TL. Influence of bone composition and apparent density on fracture toughness of the human femur and tibia. Bone. 1998;22(1):79–84.

36. Malik CL, Stover SM, Martin RB, Gibeling JC. Equine cortical bone exhibits rising R-curve fracture mechanics. J Biomech. 2003;36(2):191–8.
37. Nalla RK, Kruzic JJ, Kinney JH, Ritchie RO. Mechanistic aspects of fracture and R-curve behavior in human cortical bone. Biomaterials. 2005;26(2):217–31.
38. Nalla RK, Kruzic JJ, Kinney JH, Ritchie RO. Effect of aging on the toughness of human cortical bone: evaluation by R-curves. Bone. 2004;35(6):1240–6.
39. Koester KJ, Barth HD, Ritchie RO. Effect of aging on the transverse toughness of human cortical bone: Evaluation by R-curves. J Mech Behav Biomed Mater. 2011;4(7):1504–13.
40. Vashishth D, Behiri JC, Bonfield W. Crack growth resistance in cortical bone: concept of microcrack toughening. J Biomech. 1997;30(8):763–9.
41. Vashishth D, Tanner KE, Bonfield W. Experimental validation of a microcracking-based toughening mechanism for cortical bone. J Biomech. 2003;36(1):121–4.
42. Nalla RK, Kinney JH, Ritchie RO. Mechanistic fracture criteria for the failure of human cortical bone. Nat Mater. 2003;2(3):164–8.
43. • Zimmermann EA, Schaible E, Bale H, et al.: Age-related changes in the plasticity and toughness of human cortical bone at multiple length scales. Proc Natl Acad Sci U S A 2011, 108(35): 14416–14421. *Analzying contributors from the submicrostructure to fracture toughness of bone by X-ray diffraction, this study provides evidence that nonenzymatic collagen crosslinking lowers fibril strain, thereby reducing resistance to crack propagation.*
44. Ritchie RO: How does human bone resist fracture? Annals of the New York Academy of Sciences 2010, 1192(72–80).
45. Wang X, Shen X, Li X, Agrawal CM. Age-related changes in the collagen network and toughness of bone. Bone. 2002;31(1):1–7.
46. Tang SY, Vashishth D. The relative contributions of non-enzymatic glycation and cortical porosity on the fracture toughness of aging bone. J Biomech. 2011;44(2):330–6.
47. Hansma P, Turner P, Drake B, et al. The bone diagnostic instrument II: indentation distance increase. The Review of scientific instruments. 2008;79(6):064303.
48. •• Diez-Perez A, Guerri R, Nogues X, et al.: Microindentation for in vivo measurement of bone tissue mechanical properties in humans. J Bone Miner Res 2010, 25(8): 1877–1885. *In a small cohort, a direct measurement of the resistance to microindentation by bone tissue (five separate 200 micron spots on the tibia midshaft) was found to discriminate those with an osteoporotic fracture from age-matched subjects without a fracture.*
49. Mori S, Burr DB. Increased intracortical remodeling following fatigue damage. Bone. 1993;14(2):103–9.
50. Verborgt O, Gibson GJ, Schaffler MB. Loss of osteocyte integrity in association with microdamage and bone remodeling after fatigue in vivo. J Bone Miner Res. 2000;15(1):60–7.
51. Schaffler MB, Choi K, Milgrom C. Aging and matrix microdamage accumulation in human compact bone. Bone. 1995;17 (6):521–5.
52. Mori S, Harruff R, Ambrosius W, Burr DB. Trabecular bone volume and microdamage accumulation in the femoral heads of women with and without femoral neck fractures. Bone. 1997;21 (6):521–6.
53. Diab T, Sit S, Kim D, et al. Age-dependent fatigue behaviour of human cortical bone. Eur J Morphol. 2005;42(1–2):53–9.
54. Zioupos P, Gresle M, Winwood K: Fatigue strength of human cortical bone: Age, physical, and material heterogeneity effects. J Biomed Mater Res A 2007.
55. Norman TL, Wang Z. Microdamage of human cortical bone: incidence and morphology in long bones. Bone. 1997;20(4):375–9.
56. Nyman JS, Makowski AJ, Patil CA, et al. Measuring Differences in Compositional Properties of Bone Tissue by Confocal Raman Spectroscopy. Calcif Tissue Int. 2011;89(2):111–22.
57. Nyman JS, Roy A, Acuna RL, et al. Age-related effect on the concentration of collagen crosslinks in human osteonal and interstitial bone tissue. Bone. 2006;39(6):1210–7.
58. • Busse B, Djonic D, Milovanovic P, et al.: Decrease in the osteocyte lacunar density accompanied by hypermineralized lacunar occlusion reveals failure and delay of remodeling in aged human bone. Aging Cell 2010, 9(6): 1065–1075. *Using quantitative backscattered electron imaging and histomorphometry, this study found that the number of osteocyte lacunae decreased in the femoral cortex with age, and the peri-lucanar tissue tended to be hypermineralized in the bone of elderly donors.*
59. Vashishth D, Verborgt O, Divine G, et al. Decline in osteocyte lacunar density in human cortical bone is associated with accumulation of microcracks with age. Bone. 2000;26(4):375–80.
60. Chan KS, Chan CK, Nicolella DP. Relating crack-tip deformation to mineralization and fracture resistance in human femur cortical bone. Bone. 2009;45(3):427–34.
61. Miller E, Delos D, Baldini T, et al. Abnormal mineral-matrix interactions are a significant contributor to fragility in oim/oim bone. Calcif Tissue Int. 2007;81(3):206–14.
62. Uveges TE, Kozloff KM, Ty JM, et al. Alendronate treatment of the brtl osteogenesis imperfecta mouse improves femoral geometry and load response before fracture but decreases predicted material properties and has detrimental effects on osteoblasts and bone formation. J Bone Miner Res. 2009;24(5):849–59.
63. Dong XN, Zoghi M, Ran Q, Wang X. Collagen mutation causes changes of the microdamage morphology in bone of an OI mouse model. Bone. 2010;47(6):1071–5.
64. Oxlund H, Barckman M, Ortoft G, Andreassen TT. Reduced concentrations of collagen cross-links are associated with reduced strength of bone. Bone. 1995;17(4 Suppl):365S–71.
65. Shiraki M, Kuroda T, Tanaka S, et al. Nonenzymatic collagen cross-links induced by glycoxidation (pentosidine) predicts vertebral fractures. J Bone Miner Metab. 2008;26(1):93–100.
66. •• Gineyts E, Munoz F, Bertholon C, et al.: Urinary levels of pentosidine and the risk of fracture in postmenopausal women: the OFELY study. Osteoporos Int 2009. 21(2): 243–50. *In a cohort of French postmenopausal women (OFELY), the incidence of fracture was higher for those with urinary pentosidine levels in the highest quartile, but pentosidine was not an independent risk factor for hip and vertebral fracture with respect to age.*
67. Schwartz AV, Garnero P, Hillier TA, et al. Pentosidine and increased fracture risk in older adults with type 2 diabetes. J Clin Endocrinol Metab. 2009;94(7):2380–6.
68. Yamamoto M, Yamaguchi T, Yamauchi M, et al. Serum pentosidine levels are positively associated with the presence of vertebral fractures in postmenopausal women with type 2 diabetes. J Clin Endocrinol Metab. 2008;93(3):1013–9.
69. Silva MJ, Brodt MD, Lynch MA, et al. Type 1 diabetes in young rats leads to progressive trabecular bone loss, cessation of cortical bone growth, and diminished whole bone strength and fatigue life. J Bone Miner Res. 2009;24(9):1618–27.
70. Nyman JS, Even JL, Jo CH, et al. Increasing duration of type 1 diabetes perturbs the strength-structure relationship and increases brittleness of bone. Bone. 2011;48(4):733–40.
71. Fantner GE, Hassenkam T, Kindt JH, et al. Sacrificial bonds and hidden length dissipate energy as mineralized fibrils separate during bone fracture. Nat Mater. 2005;4(8):612–6.
72. Fantner GE, Adams J, Turner P, et al. Nanoscale ion mediated networks in bone: osteopontin can repeatedly dissipate large amounts of energy. Nano Lett. 2007;7(8):2491–8.
73. Thurner PJ, Chen CG, Ionova-Martin S, et al. Osteopontin deficiency increases bone fragility but preserves bone mass. Bone. 2010;46 (6):1564–73.
74. Sroga GE, Karim L, Colon W, Vashishth D: Biochemical characterization of major bone-matrix proteins using nanoscale-size

bone samples and proteomics methodology. Mol Cell Proteomics 2011, 10(9): M110 006718.
75. Nyman JS, Roy A, Shen X, et al. The influence of water removal on the strength and toughness of cortical bone. J Biomech. 2006;39(5):931–8.
76. Wilson EE, Awonusi A, Morris MD, et al. Three structural roles for water in bone observed by solid-state NMR. Biophys J. 2006;90 (10):3722–31.
77. Nyman JS, Ni Q, Nicolella DP, Wang X. Measurements of mobile and bound water by nuclear magnetic resonance correlate with mechanical properties of bone. Bone. 2008;42(1):193–9.
78. Horch RA, Gochberg DF, Nyman JS, Does MD. Non-invasive predictors of human cortical bone mechanical properties: T(2)-discriminated H NMR compared with high resolution X-ray. PLoS One. 2011;6(1):e16359.
79. Boskey AL. Assessment of bone mineral and matrix using back-scatter electron imaging and FTIR imaging. CurrOsteoporos Rep. 2006;4(2):71–5.
80. Draper ER, Morris MD, Camacho NP, et al. Novel assessment of bone using time-resolved transcutaneous Raman spectroscopy. J Bone Miner Res. 2005;20(11):1968–72.
81. Schulmerich MV, Cole JH, Kreider JM, et al. Transcutaneous Raman spectroscopy of murine bone in vivo. Appl Spectrosc. 2009;63(3):286–95.
82. Boskey AL, Moore DJ, Amling M, et al. Infrared analysis of the mineral and matrix in bones of osteonectin-null mice and their wildtype controls. J Bone Miner Res. 2003;18(6):1005–11.
83. Timlin JA, Carden A, Morris MD, et al. Raman spectroscopic imaging markers for fatigue-related microdamage in bovine bone. Anal Chem. 2000;72(10):2229–36.
84. Yerramshetty JS, Akkus O. The associations between mineral crystallinity and the mechanical properties of human cortical bone. Bone. 2008;42(3):476–82.
85. Ager JW, Nalla RK, Breeden KL, Ritchie RO. Deep-ultraviolet Raman spectroscopy study of the effect of aging on human cortical bone. J Biomed Opt. 2005;10(3):034012.
86. Morris MD, Mandair GS. Raman assessment of bone quality. Clin Orthop. 2011;469(8):2160–9.
87. Paschalis EP, Betts F, DiCarlo E, et al. FTIR microspectroscopic analysis of human iliac crest biopsies from untreated osteoporotic bone. Calcif Tissue Int. 1997;61(6):487–92.
88. Boskey AL, Dicarlo E, Paschalis E, et al. Comparison of mineral quality and quantity in iliac crest biopsies from high- and low-turnover osteoporosis: an FT-IR microspectroscopic investigation. Osteoporos Int. 2005;16(12):2031–8.
89. Gourion-Arsiquaud S, Faibish D, Myers E, et al. Use of FTIR spectroscopic imaging to identify parameters associated with fragility fracture. J Bone Miner Res. 2009;24(9):1565–71.
90. Gourion-Arsiquaud S, Allen MR, Burr DB, et al. Bisphosphonate treatment modifies canine bone mineral and matrix properties and their heterogeneity. Bone. 2010;46(3):666–72.
91. Paschalis EP, Glass EV, Donley DW, Eriksen EF. Bone mineral and collagen quality in iliac crest biopsies of patients given teriparatide: new results from the fracture prevention trial. J Clin Endocrinol Metab. 2005;90(8):4644–9.
92. McCreadie BR, Morris MD, Chen TC, et al. Bone tissue compositional differences in women with and without osteoporotic fracture. Bone. 2006;39(6):1190–5.
93. Balooch G, Balooch M, Nalla RK, et al. TGF-beta regulates the mechanical properties and composition of bone matrix. Proc Natl Acad Sci U S A. 2005;102(52):18813–8.
94. Chang JL, Brauer DS, Johnson J, et al. Tissue-specific calibration of extracellular matrix material properties by transforming growth factor-beta and Runx2 in bone is required for hearing. EMBO reports. 2010;11(10):765–71.
95. Mohammad KS, Chen CG, Balooch G, et al. Pharmacologic inhibition of the tgf-Beta type I receptor kinase has anabolic and anti-catabolic effects on bone. PLoS One. 2009;4(4): e5275.
96. Edwards JR, Nyman JS, Lwin ST, et al. Inhibition of TGF-beta signaling by 1D11 antibody treatment increases bone mass and quality in vivo. J Bone Miner Res. 2010;25(11):2419–26.
97. • Nyman JS, Lynch CC, Perrien DS, et al.: Differential effects between the loss of MMP-2 and MMP-9 on structural and tissue-level properties of bone. J Bone Miner Res 2011, 26(6): 1252–1260. *In an assessment of bones from wild-type and genetic knockout mice, this study found that the loss of MMP-2 decreased bone strength, whereas the loss of MMP-9 decreased bone toughness, thereby suggesting that matrix processing proteins are important to the fracture resistance of bone.*
98. Elefteriou F, Benson MD, Sowa H, et al. ATF4 mediation of NF1 functions in osteoblast reveals a nutritional basis for congenital skeletal dysplasiae. Cell Metab. 2006;4(6):441–51.
99. Wang W, Nyman JS, Moss HE, et al. Local low-dose lovastatin delivery improves the bone-healing defect caused by Nf1 loss of function in osteoblasts. J Bone Miner Res. 2010;25(7):1658–67.
100. Wang W, Nyman JS, Ono K, et al. Mice lacking Nf1 in osteochondroprogenitor cells display skeletal dysplasia similar to patients with neurofibromatosis type I. Hum Mol Genet. 2011;20(20):3910–24.

THE JOURNAL OF BIOLOGICAL CHEMISTRY VOL. 287, NO. 43, pp. 35975–35984, October 19, 2012
Published in the U.S.A.

Transforming Growth Factor β Suppresses Osteoblast Differentiation via the Vimentin Activating Transcription Factor 4 (ATF4) Axis*

Received for publication, April 16, 2012, and in revised form, August 31, 2012 Published, JBC Papers in Press, September 5, 2012, DOI 10.1074/jbc.M112.372458

Na Lian[‡§], Tonghui Lin[‡¶], Wenguang Liu[‡¶], Weiguang Wang[‡§], Lingzhen Li[‡¶], Stephanie Sun[‡¶], Jeffry S. Nyman[‡‖], and Xiangli Yang[‡§¶1]**

From the [‡]Vanderbilt Center for Bone Biology, the [¶]Department of Medicine, the [§]Department of Pharmacology, and the [‖]Department of Orthopedics and Rehabilitation, Vanderbilt University Medical Center, Nashville, Tennessee 37232 and the [**]Department of Veteran Affairs, Tennessee Valley Health Care System, Nashville, Tennessee 37212

Background: Transforming growth factor β (TGFβ) inhibits *osteocalcin* (*Ocn*) transcription and osteoblast differentiation.
Results: The inhibition of *Ocn* expression and osteoblast differentiation by TGFβ is blunted upon lack of *Atf4* or *vimentin* knockdown.
Conclusion: ATF4 and vimentin are novel downstream targets of TGFβ in osteoblasts.
Significance: Understanding mechanisms by which transcription factors are regulated is crucial for developing effective anabolic drugs for bone.

ATF4 is an osteoblast-enriched transcription factor of the leucine zipper family. We recently identified that vimentin, a leucine zipper-containing intermediate filament protein, suppresses ATF4-dependent *osteocalcin* (*Ocn*) transcription and osteoblast differentiation. Here we show that TGFβ inhibits ATF4-dependent activation of *Ocn* by up-regulation of vimentin expression. Osteoblasts lacking *Atf4* (*Atf4*$^{-/-}$) were less sensitive than wild-type (WT) cells to the inhibition by TGFβ on alkaline phosphatase activity, *Ocn* transcription and mineralization. Importantly, the anabolic effect of a monoclonal antibody neutralizing active TGFβ ligands on bone in WT mice was blunted in *Atf4*$^{-/-}$ mice. These data establish that ATF4 is required for TGFβ-related suppression of *Ocn* transcription and osteoblast differentiation *in vitro* and *in vivo*. Interestingly, TGFβ did not directly regulate the expression of ATF4; instead, it enhanced the expression of vimentin, a negative regulator of ATF4, at the post-transcriptional level. Accordingly, knockdown of endogenous *vimentin* in 2T3 osteoblasts abolished the inhibition of *Ocn* transcription by TGFβ, confirming an indirect mechanism by which TGFβ acts through vimentin to suppress ATF4-dependent *Ocn* activation. Furthermore, inhibition of PI3K/Akt/mTOR signaling, but not canonical Smad signaling, downstream of TGFβ, blocked TGFβ-induced synthesis of vimentin, and inhibited ATF4-dependent *Ocn* transcription in osteoblasts. Thus, our study identifies that TGFβ stimulates vimentin production via PI3K-Akt-mTOR signaling, which leads to suppression of ATF4-dependent *Ocn* transcription and osteoblast differentiation.

Transforming growth factor β (TGFβ)[2] regulates many biological processes including patterning during development, cell proliferation, differentiation, apoptosis, and other physiological and pathological conditions such as wound healing, fibrosis, and cancer growth and metastasis. In the mammalian skeleton, TGFβ is one of the most abundant cytokines stored in bone matrix; and once activated from its latent form, it promotes osteoblast proliferation and mesenchymal stem cell recruitment to active bone remodeling sites (1–5), while inhibits osteoblast differentiation (6–8). The canonical Smad-dependent signaling has been identified as a mediator of TGFβ in skeletal cells as well as in many other cell types. In response to ligand binding, TGFβ receptors phosphorylate Smad2 and/or Smad3, which in turn bind to Smad4 to induce translocation into the nucleus (9), where the Smad complex either binds directly to DNA or indirectly to other transcription factors to regulate gene transcription (10).

It has become clear now that multiple Smad-independent or noncanonical signaling pathways are activated in response to TGFβ ligands in various cell types. These include: MAP kinase (MAPK) pathways in intestine, lung epithelial cells, and breast cancer cells; Rho-like GTPase signaling pathways during epithelial to mesenchymal transition (EMT) in epithelial cells and primary keratinocytes; and mammalian targets of rapamycin (mTOR) through phosphatidylinositol 3-kinase (PI3K) and Akt pathways during EMT in fibroblasts (11–18). Although each of these signaling pathways has been shown to play an important role in skeletal biology, whether TGFβ activates non-canonical signaling pathways in osteoblasts is unknown.

Activating transcription factor (ATF4) is a leucine zipper-containing transcription factor belonging to the CREB family

* This work was supported by the Vanderbilt University career developmental funds (to X. Y.) and the Dept. of Veterans Affairs, Biomedical Laboratory Research and Development (to J. S. N.).
[1] To whom correspondence should be addressed: 2215B Garland Ave., 1225F MRB IV, Nashville, TN 37232-0575. Tel.: 615-322-8052; Fax: 615 343 2611; E-mail: xiangli.yang@vanderbilt.edu.

[2] The abbreviations used are: TGFβ, transforming growth factor β; EMT, epithelial to mesenchymal transition; ATF, activating transcription factor; mTOR, mammalian targets of rapamycin; *Ocn*, *osteocalcin;* μCT, microcomputed tomography; HA, hydroxyapatite; HDAC, histone deacetylase; PTH, parathyroid hormone.

and was originally identified as an osteoblast-specific transcription factor required for *osteocalcin* (*Ocn*) transcription and osteoblast differentiation (19). *Ocn* mRNA is exclusively expressed in differentiated osteoblasts hence it is often used as a marker gene of mature osteoblasts (20). Together with Runx2, the first reported osteoblast-specific transcription factor, ATF4 activates *Ocn* transcription *in vitro* and *in vivo* through direct binding to its cognate osteoblast-specific element 1 (OSE1) of the *Ocn* promoter (19, 21, 22). In osteoblasts, TGFβ targets Runx2 via a canonical Smad signaling pathway to achieve its inhibition of both *Runx2* and *Ocn* transcription, thereby suppressing osteoblast differentiation (6). However, it is possible that TGFβ targets other effectors at the transcriptional level to inhibit *Ocn* transcription in osteoblasts.

We have recently identified that in osteoblasts vimentin binds directly to ATF4 through its first leucine-zipper domain, which prevents ATF4 from binding to its cognate DNA OSE1 on the *Ocn* promoter, leading to inhibition of ATF4-dependent *Ocn* transcription and osteoblast differentiation (23). Vimentin is a member of the intermediate filament protein family and the most widely accepted molecular marker of mesenchymal cells. Moreover, its mRNA is often up-regulated in response to TGFβ during EMT and cancer progression (24, 25). Consistent with its inhibitory role during osteoblast differentiation, vimentin expression is down-regulated when osteoblasts progress toward a fully differentiated stage (23). Since this suggested that one component of vimentin regulation involves the regulatory control of its expression, we searched for the extracellular ligands that govern its expression. In doing so, we noticed that TGFβ stimulated *vimentin* mRNA in C2C12 myoblastic cells (26), a cell type of mesenchymal origin that can differentiate into chondrocytes and osteoblasts (27). Given that TGFβ and vimentin both negatively regulate *Ocn* transcription and osteoblast differentiation, we hypothesized that TGFβ targets vimentin and ATF4 to suppress *Ocn* transcription and osteoblast differentiation.

Here we present evidence that TGFβ requires endogenous ATF4 to inhibit *Ocn* transactivation in primary osteoblasts and osteoblastic cell lines. With the delivery of a monoclonal anti-TGFβ antibody to mice, we show that ATF4 is also required for TGFβ to increase bone mass. Employing a series of molecular and biochemical approaches, we demonstrate that TGFβ directly up-regulates vimentin production at post-transcriptional level, via PI3K-Akt-mTOR signaling, but not Smad signaling, to achieve its inhibition of *Ocn* transcription. Therefore, our study identifies two novel effectors, vimentin and ATF4, that act downstream of TGFβ in the regulation of osteoblast differentiation via PI3K-Akt-mTOR signaling.

EXPERIMENTAL PROCEDURES

Materials—Tissue culture media and fetal bovine serum were purchased from Invitrogen. Anti-vimentin antibodies were from Santa Cruz Biotechnology and Biovision for V9 anti-rat vimentin and anti-mouse vimentin (#3634), respectively. Antibodies for ATF4 (C20) and Sp1 (PEP2) were from Santa Cruz Biotechnology, HA tag was from Abcam (ab9110); Flag tag was from Sigma (M2); and phospho-Smad2/3 was from Cell Signaling. Recombinant human (rh) TGFβ1 is from R&D systems. All chemicals were from Sigma unless indicated otherwise.

Cell Culture—ROS17/2.8 rat osteosarcoma cells were grown in DMEM/F-12 medium containing 10% FBS. Mouse osteoblastic 2T3 and MC3T3-E1 cell lines were cultured in α-Minimal Essential Medium (αMEM) containing 10% FBS. C2C12 myoblasts were grown in Dulbecco's modified Eagle's medium (DMEM) that contains 10% FBS and myoblastic DMEM or differentiation medium that contains 2% horse serum. COS1 monkey kidney cells were cultured in DMEM containing 10% FBS. All media were supplemented with 1% penicillin-streptomycin, and cells were passaged every 3 days.

Northern Blot Hybridization—Total RNA from indicated sources was isolated using TRIzol (Invitrogen) according to the manufacturer's protocols. Total RNA (5 μg) was resolved in 1% agarose gel and transferred onto nylon membranes. After crosslinking with UV light, the membranes were hybridized in 6× SSC buffer at 60 °C overnight with the following probes: partial cDNA of mouse *vimentin* from 792 to 1218, mouse *Atf4* covering 287 nucleotides of 5′-untranslated region and 180 nucleotides of coding region, full-length mouse *Ocn gene 2*, and mouse *Gapdh* cDNAs.

Establishment of Permanent Reporter Cells—ROS17/2.8 cells were seeded at a density of 5×10^5 cells/well in 6-well culture dishes, and reporter construct (1 μg) of p6×OSE1-Luc, p6×mOSE1-Luc, or negative control p3xAP1-Luc was cotransfected with pcDNA3.1(+) (20 ng) at 50:1 ratio using Lipofectamine (Invitrogen) 18 h later. Cells were then allowed to grow to confluence. Neomycin (G418)-resistant colonies were then selected with G418 (300 μg/ml)-containing culture medium and pooled for experimental use.

Transient DNA Transfection and Luciferase Assay—COS1 cells were seeded at a density of 2.5×10^5/well in 6-well culture dishes for 20 h and then transfected with 2 μg/well of Flag-ATF4 or HA-vimentin expression plasmid. For reporter assays, cells were plated in 24-wells at a density of 2.5×10^4/well. p6×OSE1-Luc (0.25 μg/well) together with 0.05 μg/well of β-galactosidase (β-gal) were transfected into COS1 cells using Lipofectamine (Invitrogen). Cells were lysed 24 h post DNA transfection, and the luciferase and β-gal activity was measured using cell lysate. Fold activation or inhibition of luciferase activity was calculated by normalization of luciferase activity with β-gal activity. For v*imentin* knockdown, 2T3 osteoblastic cells were plated in 6-well culture dishes at 2.5×10^5/well and then transiently cotransfected with *psiRNA* (1 μg/well) empty vector or *psiRNA-Vim* with indicated reporter constructs (1 μg/well).

Primary Calvarial Osteoblast Isolation and Osteoblast Differentiation Assay—Calvariae were collected from neonatal (P3) pups, pressed on Science Brand Kimwipes to remove blood and surrounding tissues, cleaned with 1× PBS, and then subjected to series of collagenase digestions as described previously (28). Cells released from the first 2 digestions were discarded to enrich the numbers of osteoblastic cells. Cells released from the third digestion were plated in αMEM containing 10% FBS until confluence, which was defined as passage 0.

For differentiation assays, primary cells from passage 1 or osteoblastic cell lines were grown in 24-well plates in αMEM supplemented with 5 mM β-glycerophosphate and 100 μg/ml

ascorbic acid for either 2 or 12 days for alkaline phosphatase staining or von Kossa staining, respectively, as previously described (29).

2G7 Treatment—Ten pairs of 10-week-old WT and *Atf4*$^{-/-}$ littermates were treated with anti-TGFβ monoclonal antibody 2G7 or control IgG at 10 mg/kg. The intraperitoneal injections of each antibody were administered 3 times per week for 4 weeks (30).

Micro-computed Tomography (μCT) Analysis—Mouse femurs were collected and fixed overnight in 4% PFA (pH 7.4) and then 70% ethanol. Trabecular bone of the metaphysis was evaluated using an *ex vivo* μCT imaging system (Scanco μCT40; Scanco Medical, Bassersdorf, Switzerland). Each femur was fit into a specimen tube and aligned with the scanning axis. Tomographic images were acquired at 55 kV and 145 mA with an isotropic voxel size of 12 μm, and at an integration time of 250 ms with 500 projections collected per 180 °C rotation. For 100 slices proximal to the growth plate, contours were fit to the inner layer of the cortical bone to define the total tissue volume (TV). Applying a Gaussian noise filter with a variance of 0.8 and support of 1 as well as a threshold of 300 mg of hydroxyapatite (HA) per cm^3 to distinguish mineralized from non-mineralized tissue for each femur scan, we quantified the volume of trabecular bone tissue (BV) per TV (BV/TV) as well as volumetric density (in mgHA/cm3) of the bone-mineralized tissue (BMD) (31).

Western Blot Analysis—Total cell lysates from indicated cell types were isolated with radioimmunoprecipitation assay (RIPA) buffer containing 50 mM Tris-Cl, pH 7.6, 150 mM NaCl, 0.1% SDS, 0.5% sodium deoxycholate, 1% Nonidet P-40, and protease inhibitors (Complete ULTRA Protease Inhibitor Mixture Tablets, Roche Applied Science). Nuclear extracts were isolated using high-salt nuclear extraction buffer on hypotonic buffer-swelled cells as described (32). Total cellular proteins or nuclear extracts (50 μg per lane) were loaded onto 10% SDS-PAGE and Western blots were performed following standard protocols. Antibody concentrations were 0.5–1 μg/ml.

TGFβ and Inhibitor Treatment—ROS17/2.8 cells, primary rat or mouse calvarial osteoblasts, in 60-mm plates at 90% confluent, were starved in serum-free media overnight. rhTGFβ1 (0.2∼2 ng/ml) or vehicle (4 mM HCl containing 1 mg/ml BSA) was then added to the cell culture medium containing 1% FBS, and cells were incubated for an additional 5–6 h. For inhibitor treatment, MG115 (Piptide Institute Inc. Japan), SB505124 (Sigma), cycloheximide (Sigma), wortmannin (EMD4Biosciences), or rapamycin (EMD4 Biosciences) at indicated concentrations (0.1 nM to 5 nM) were pre-incubated with cells for 30 min prior to adding TGFβ.

Statistics—Data are presented as mean ± S.D. Statistical analyses were performed using Student's *t* test. All *in vitro* experiments were repeated at least three times.

RESULTS

ATF4 Is Required for TGFβ to Inhibit Osteoblast Differentiation—To investigate whether ATF4 was downstream of TGFβ, we first established stable ROS17/2.8 cell lines carrying a reporter luciferase gene driven by 6 repeats of wild type (WT) ATF4 binding element OSE1, p6xOSE1-Luc. As controls, we also made two other stable cell lines carrying a luciferase gene driven by either 6 repeats of a mutant ATF4 binding element, p6xmOSE1-Luc to which ATF4 fails to bind (21), or 3 repeats of the activating protein 1 (AP1) binding element, p3xAP1-Luc. Treatment of these reporter cell lines with rhTGFβ1 at various concentrations, ranging from 0.2 to 2 ng/ml, inhibited dose-dependently luciferase activity driven by 6xOSE1, but not by 6xmOSE1 (Fig. 1, *A* and *B*), indicating that the inhibitory effect of TGFβ on ATF4-dependent *Ocn* promoter activity relies on ATF4 binding to its cognate DNA. Furthermore, TGFβ inhibition is specific to the *Ocn* promoter and not a general phenomenon of leucine zipper-containing transcription factors since TGFβ failed to reduce luciferase activity in reporter cells driven by AP1 DNA binding element repeats (Fig. 1*C*).

To determine whether ATF4 was necessary for TGFβ to suppress endogenous *Ocn* expression and osteoblast differentiation, we utilized the *Atf4*-deficient (*Atf4*$^{-/-}$) mouse model (33). Freshly isolated primary calvarial osteoblasts (passage 1) from wild type (WT) and *Atf4*$^{-/-}$ pups were treated with rhTGFβ1 (0.5 ng/ml) under osteogenic induction media for 10 days, and total RNA was collected for qRT-PCR analyses. Our data showed that TGFβ inhibited endogenous *Ocn* expression by 86% in WT calvarial osteoblasts but only by 43% in *Atf4*$^{-/-}$ calvarial osteoblasts (Fig. 1*D*). Consistent with this observation, TGFβ reduced alkaline phosphatase (ALP) activity in WT control cells by 46% but had no such effect in *Atf4*$^{-/-}$ calvarial cells (Fig. 1*E*). Lastly, low doses of TGFβ (0.1 and 0.2 ng/ml) decreased the number of mineralized nodule formation by 90% in WT but only 20% in *Atf4*$^{-/-}$ calvarial osteoblasts (Fig. 1*F*). Collectively, these data indicate that lack of endogenous ATF4 attenuates the potency of TGFβ to inhibit endogenous *Ocn* expression, ALP activity and differentiation or mineralization of osteoblasts *in vitro*.

To address whether ATF4 was also required for TGFβ *in vivo* and because treatment of WT mice with 1D11 an anti-TGFβ monoclonal antibody blocking all three isoforms of TGFβ (34), increased trabecular bone volume fraction in mice (30), we treated WT and *Atf4*$^{-/-}$ mice with 2G7, an monoclonal antibody with similar reactivity to the 1D11 (35). WT control and *Atf4*$^{-/-}$ mice were injected intraperitoneally with a TGFβ monoclonal antibody 2G7 for 4 weeks. Consistent with the results reported previously using 1D11 (30), μCT analysis revealed that 2G7 treatment increased bone volume fraction in WT mice by more than 30%, however, it could not improve the low bone mass in *Atf4*$^{-/-}$ mice (Fig. 1, *G* and *H*). Thus, these results confirmed that ATF4 is an important molecule downstream of TGFβ *in vivo*.

TGFβ Stimulates Vimentin Post-transcriptionally in Osteoblasts—To determine whether TGFβ suppressed ATF4-dependent activation of *Ocn* and osteoblast differentiation (Fig. 1) via a direct effect on ATF4, we then analyzed whether TGFβ inhibited ATF4 expression. Primary calvarial osteoblasts (passage 1) were treated for 10 days with rhTGFβ1 at concentrations of 0.2, 1, or 2 ng/ml under osteogenic culture conditions, and then total RNA and protein were analyzed. As expected, endogenous *Ocn* expression decreased whereas ATF4 expression slightly increased, in response to TGFβ in a dose-depen-

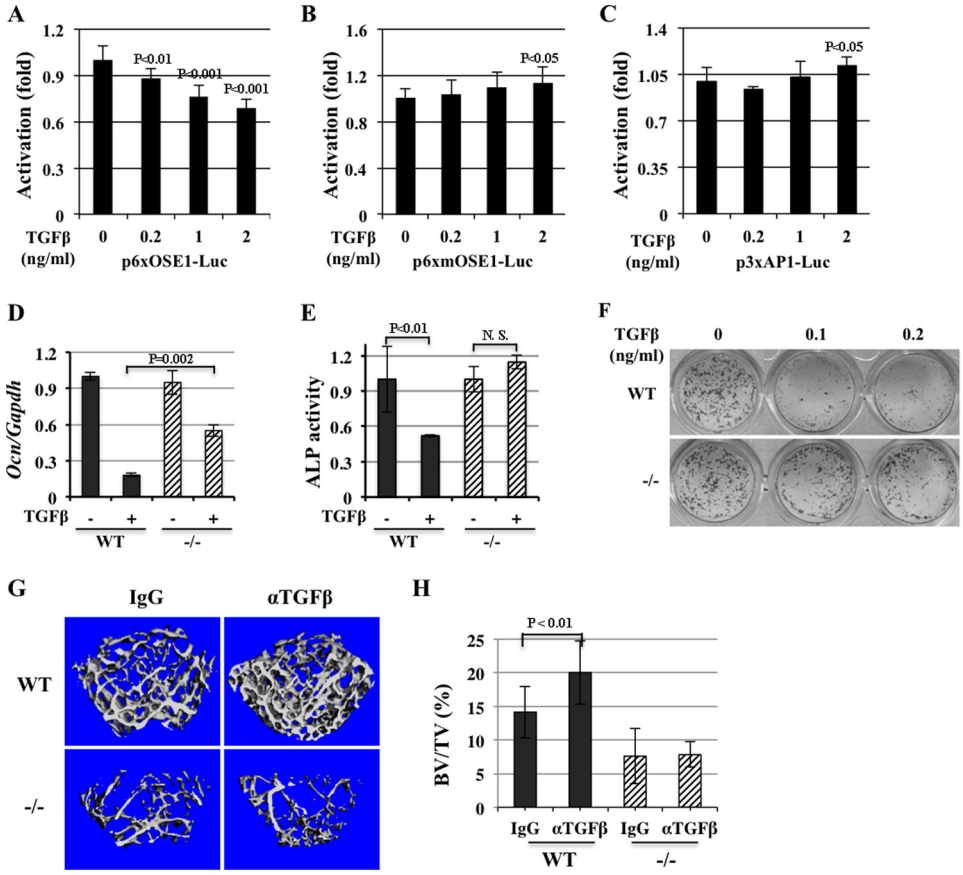

FIGURE 1. **ATF4 is required for TGFβ to inhibit *osteocalcin (Ocn)* transcription.** *A–C*, TGFβ inhibits ATF4-dependent reporter activity. Luciferase activity is decreased by treatment of rhTGFβ1 at indicated concentrations in stable ROS17/2.8 reporter cells. p6xOSE1-Luc, luciferase gene driven by 6 repeats of ATF4-binding elements reporter (*A*); p6xmOSE1-Luc, 6 repeats of mutant ATF4-binding element driving luciferase reporter (*B*); p3xAP1-Luc, 3 repeats of unrelated leucine-zipper protein AP1-binding site- driven reporter (*C*). *D*, inhibition of endogenous *Ocn* expression by TGFβ is attenuated in *Atf4*$^{-/-}$ calvarial osteoblasts. Quantitative RT-PCR (qRT-PCR) analysis of total RNA isolated from WT and *Atf4*$^{-/-}$ calvalrial osteoblasts treated with vehicle (−) or rhTGFβ1 (+, 0.5 ng/ml) in osteogenic medium for 10 days. Note that TGFβ decreased endogenous *Ocn mRNA* level in WT calvarial osteoblasts, which was attenuated (48% inhibition) in *Atf4*$^{-/-}$ mutant osteoblasts. *E*, TGFβ reduced alkaline phosphatase (ALP) activity in WT but not in *Atf4*$^{-/-}$ osteoblasts. ALP assay of WT and *Atf4*$^{-/-}$ calvarail osteoblasts treated with vehicle (−) or rhTGFβ (+, 0.5 ng/ml) in osteogenic medium for 2 days. *F*, TGFβ inhibits mineralized nodule formation in WT but not in A*tf4*$^{-/-}$ osteoblasts. von Kossa staining of calvarial osteoblasts treated with rhTGFβ1 (0.5 ng/ml) in osteogenic medium for 10 days. Note that TGFβ reduced the number of mineralized nodules (*black colonies*) dramatically (>90%) in the WT cultures but only slightly in *Atf4*$^{-/-}$ osteoblasts (<20%). *G*, ATF4 is required for the anabolic effect of anti-TGFβ antibody *in vivo*. μCT analysis of trabecular bones of WT and *Atf4*$^{-/-}$ femurs treated with control IgG antibody or anti-TGFβ monoclonal antibody (2G7, αTGFβ) neutralizing three forms of TGFβ ligand for 4 weeks. *H*, quantification of data shown in *G*. Note that 2G7 treatment increased trabecular bone volume (*BV*) *versus* total tissue volume (BV/TV) in WT femurs by 30% but failed to rescue the low BV/TV in *Atf4*$^{-/-}$ femur. $n = 6$.

dent manner (Fig. 2, *A* and *B*). These results suggested that the suppression of ATF4 transcriptional activity by TGFβ is not due to a decrease in the level of ATF4 but may be via an indirect mechanism.

One of the candidates was vimentin, because we recently found that it acted as a suppressor of ATF4 in osteoblasts (23) and others have shown that its expression was stimulated by TGFβ (26). To address whether vimentin was the mediator linking TGFβ signaling and ATF4, we first treated ROS 17/2.8 cells with TGFβ and found it could induce vimentin protein expression dose-dependently. Surprisingly, however, TGFβ did not increase *vimentin* mRNA expression at all of the concentrations tested (Fig. 2, *C* and *D*). These data indicated that in osteoblasts TGFβ regulates vimentin expression at the protein level and not at the mRNA level, which was different from what had been observed in C2C12 cells previously (26). To further verify our findings, we also treated a panel of osteoblasts along with C2C12 cells (as a positive control) with low dose rhTGFβ1 (0.2 ng/ml), which significantly suppressed WT primary osteoblast differentiation *in vitro* (Fig. 1*F*). The results indicated that TGFβ increased vimentin protein level but not its mRNA level in all tested cells, including mouse primary bone marrow stromal cells (BMSC), calvarial osteoblasts (POB), the 2T3 mouse preosteoblastic cells, and the MC3T3-E1 mouse committed osteoblasts. However and consistent with previous report (26), TGFβ in the C2C12 cells increased both protein and mRNA vimentin levels (Fig. 2, *E* and *F*). Thus, these data demonstrated that TGFβ up-regulates vimentin expression at the post-transcriptional level in osteoblasts.

Vimentin Is Required for TGFβ to Inhibit Ocn Expression—To understand whether vimentin played an essential role in mediating the inhibitory effect of TGFβ on ATF4 transcriptional activity and *Ocn* transcription, we knocked down endogenous *vimentin* expression in 2T3 mouse osteoblastic cells by transfection with *siRNA-Vim* (23) and the p6xOSE1-Luc as a readout for ATF4 transcriptional activity, and then tested their response to TGFβ by reporter assays. 2T3 mouse cells instead of primary osteoblasts were used to ensure the transfection effi-

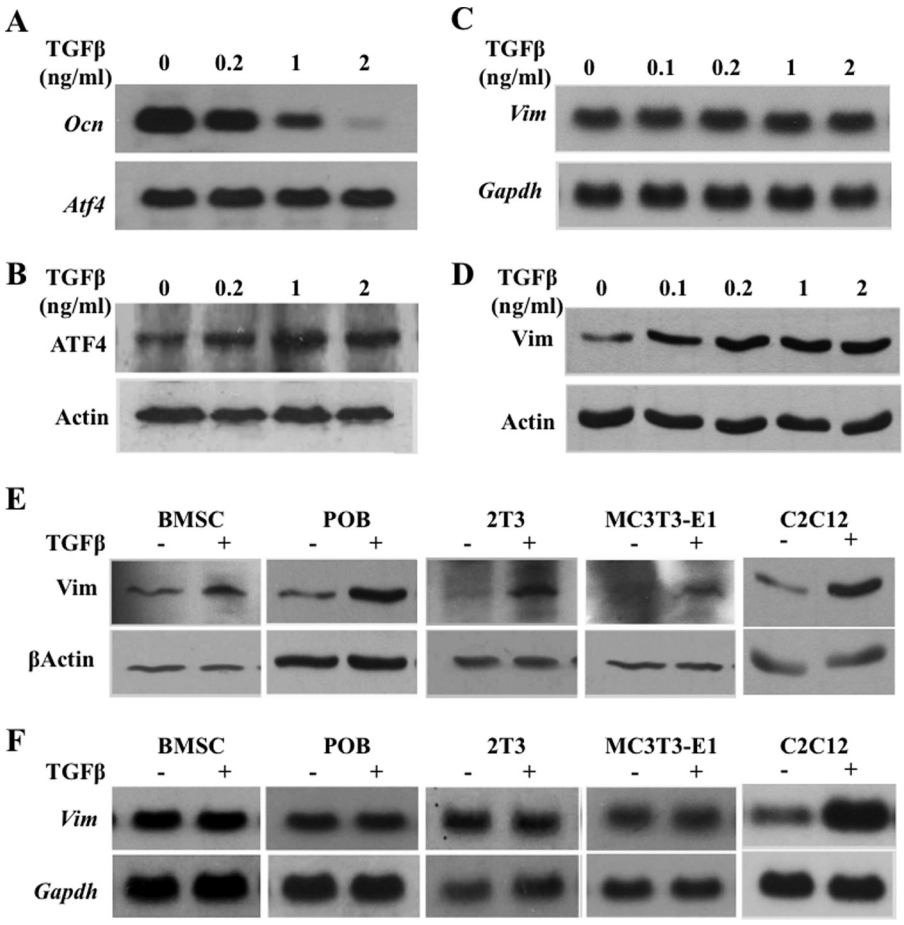

FIGURE 2. **TGFβ inhibits *Ocn* expression and stimulates vimentin expression post-transcriptionally.** *A*, Northern blot analysis of total RNA from primary calvarial osteoblasts showing that TGFβ inhibits endogenous *Ocn* expression dose-dependently. *B*, Western blot analysis of total protein from primary calvarial osteoblasts. *C*, Northern blot analysis with indicated cDNA probes showing that TGFβ does not affect endogenous *vimemtin* mRNA level in calvarial osteoblasts. *D*, Western blot analysis showing that TGFβ stimulates vimenitn protein in calvarial osteoblasts. *E*, Western blot analyses showing that rhTGFβ1 (0.2 ng/ml) stimulates vimentin protein expression in the indicated primary osteoblasts and osteoblastic cell lines. *F*, Northern blot analyses showing that rhTGFβ1 (0.2 ng/ml) does not affect endogenous *vimentin* mRNA level in the indicated primary osteoblasts and osteoblastic cell lines.

ciency. We also transfected 2T3 cells with *siRNA* empty vector to serve as negative control cells. Fig. 3*A* (*lanes 1* and *2*), rhTGFβ1 (0.5 ng/ml) decreased luciferase activity by 36%, which was expected and consistent with what we observed previously in ROS17/2.8 reporter cells (Fig. 1*A*). Luciferase activity increased 2.7-fold in 2T3 cells transfected with *siRNA-Vim*, due to the knockdown of endogenous *vimentin* that removed its suppression of ATF4 transcriptional activity (23). When TGFβ was added to these cells, ATF4 reporter activity remained 2.5-fold higher in cells containing *siRNA-Vim* than in cells containing *siRNA* control vector (Fig. 3*A*, *lanes 3* and *4*). The knockdown of endogenous *vimentin* was confirmed by the absence of *vimentin mRNA* in *siRNA-Vim* transfected cells, which could not be rescued by rhTGFβ1. Consistent with our previous finding (23) and transfection results shown in Fig. 3*A*, a low level of endogenous *Ocn* expression in 2T3 cells transfected with *siRNA* control vector was inhibited by rhTGFβ1 (0.5 ng/ml) treatment; whereas this inhibition was blunted in cells transfected with *siRNA-Vim* (Fig. 3*B*). qRT-PCR data indicated that TGFβ1 inhibited endogenous *Ocn* expression by 60% in cells transfected with empty *siRNA* vector. As expected, vimentin knockdown in 2T3 preosteoblasts by *siRNA-Vim* increased endogenous *Ocn* expression by 4-fold, which was not affected by TGFβ1 (Fig. 3*C*). Therefore, these data validated that endogenous *vimentin* is required for TGFβ to suppress ATF4-dependent *Ocn* transcription *in vitro*.

To determine whether vimentin protein level also fluctuated *in vivo* in response to TGFβ administration, we analyzed vimentin content in the long bones of 2G7 or control antibody-treated mice. Western blot showed that 2G7 treatment decreased the abundance of endogenous vimentin in long bone lysates compared with IgG control antibody treatment while ATF4 abundance remained constant in both control and 2G7 treated long bone samples (Fig. 3*D*). Thus, these results strongly suggested that TGFβ suppresses *Ocn* transcription and osteoblast differentiation via up-regulation of vimentin expression.

An increased protein level can be attributed to increased synthesis and/or decreased degradation. To determine which of these two possibilities contributed to the TGFβ-induced accumulation of vimentin protein in osteoblasts, we tested the effects of cycloheximide, a protein synthesis inhibitor, MG115, a proteasome inhibitor, on vimentin expression. We included Flag-ATF4 as a positive control, because it accumulates in many non-osteoblastic cell lines upon MG115 treatment (36). Analysis of nuclear extracts of COS1 cells transfected with HA-vimentin or Flag-ATF4 expression vector showed that treat-

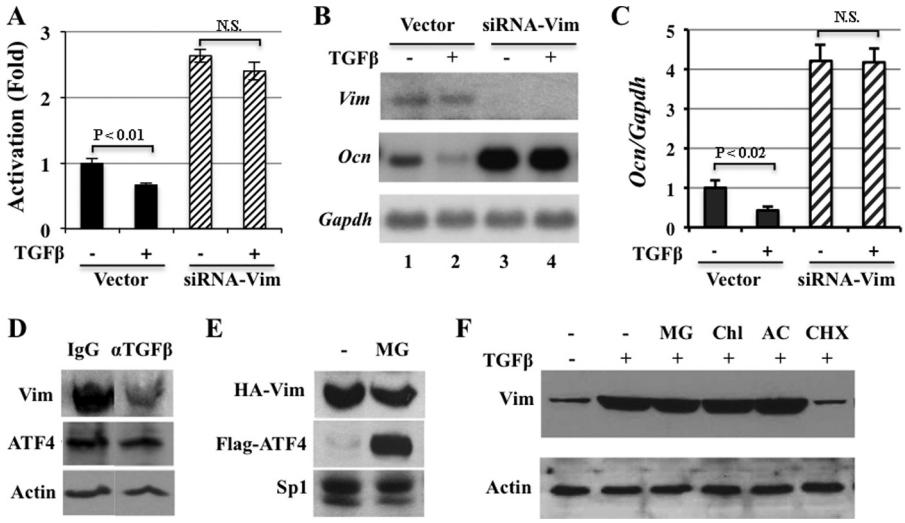

FIGURE 3. **Vimentin is required for the suppression of *Ocn* expression by TGFβ in osteoblasts.** *A*, transient DNA transfection in 2T3 preosteoblastic cells demonstrating that rhTGFβ (0.5 ng/ml) decreased luciferase activity (*lanes 1* and *2*). Note that luciferase activity increased when *siRNA-Vim* was co-transfected (*lanes 3* and *4*). *N.S.*, not statistically significant. *B*, Northern blot analysis of RNA from 2T3 osteoblastic cells transfected with *siRNA* vector or *siRNA-Vim* using indicated cDNA probes. Note that knockdown of endogenous *vimentin* by *siRNA-Vim* (*top panel*) blunted the inhibition of *Ocn* transcription by TGFβ (*middle panel*). *C*, qRT-PCR results confirming that *vimentin* knockdown by *siRNA-Vim* abolished the suppression of endogenous *Ocn* expression by rhTGFβ (0.5 ng/ml). *D*, Western blot analysis of long bone total protein extracts demonstrating that neutralizing the activity of TGFβ *in vivo* by anti-TGFβ decreases vimentin protein abundance. 10-week-old mice were treated with control antibody (*IgG*) or anti-TGFβ monoclonal antibody (*αTGFβ*) neutralizing three forms of TGFβ ligand for 4 weeks. *E*, proteasomal degradation inhibitor MG115 (*MG*) stabilizes ATF4 but not vimentin. Western blot analysis of nuclear extracts of COS1 cells transfected with expression plasmids of HA-Vim or Flag-ATF4 using anti-HA or anti-Flag antibodies. Sp1, loading control of nuclear extracts. *F*, protein synthesis is required for TGFβ to induce vimentin expression. ROS17/2.8 cells were pretreated with indicated inhibitors prior to the treatment of rhTGFβ1 (0.2 ng/ml). Note that TGFβ-induced vimentin is not affected by proteasomal inhibitor, MG115 (*MG*), or lysosomal inhibitors, chloroquine (*ChlQ*, 100 mM) and ammonium chloride (*AC*, 50 mM), but is diminished by protein translation inhibitor cycloheximide (*CHX*).

ment of MG115 (10 μg/ml) did not alter the abundance of HA-vimentin but did, as expected, increase Flag-ATF4 considerably (Fig. 3*E*). To address whether endogenous vimentin in osteoblasts behaved similarly to HA-vimentin in COS1 cells, we co-treated ROS17/2.8 cells with rhTGFβ1 (0.5 ng/ml), MG115 (10 μg/ml), or two lysosomal inhibitors chloroquine and ammonium chloride. As can be seen in Fig. 3*F*, the TGFβ-induced increase in vimentin expression was not affected by MG115, chloroquine (100 μM), or ammonium chloride (50 mM), but strongly decreased to basal level by cycloheximide (15 μg/ml). Collectively, these data indicated that protein neosynthesis is required for TGFβ to stimulate vimentin expression in osteoblasts.

PI3K-Akt-mTOR Signaling Is Required for TGFβ to Induce Vimentin Synthesis—Because TGFβ has been shown to stimulate protein translation initiation via the PI3K-Akt-mTOR signaling pathway (Fig. 4*A*, adapted from Ref. 14), we then examined whether the PI3K-Akt-mTOR and/or the canonical Smad-signaling is responsible for TGFβ to induce vimentin in osteoblasts (Figs. 2 and 3). Wortmannin, an inhibitor of Akt phosphorylation by PI3K; rapamycin (1 and 5 nM), an inhibitor of S6K phosphorylation by mTOR (14, 37–39); and SB505124, an inhibitor of Smad2/3 phosphorylation downstream of the type I TGFβ receptor (40), were used to treat ROS17/2.8 cells. Western blot demonstrated that both wortmannin and rapamycin (1 and 5 nM) drastically reduced vimentin protein expression induced by TGFβ, which correlated with a strong decrease in Akt and S6K phosphorylation. SB505124 (0.1 and 0.2 nM) effectively decreased TGFβ-induced Smad2 phosphorylation but not TGFβ-induced vimentin expression (Fig. 2, *B–D*). As expected, wortmannin and rapamycin (1 and 5 nM) did not inhibit the TGFβ-induced Smad2 phosphorylation (Fig. 4, *B--E*), demonstrating that these inhibitors do not have an off-target effect at these concentrations. Moreover, overexpression of a dominant negative form of Akt, Akt-AA (38), blocked the increase in vimentin expression induced by TGFβ, which also correlated with an inhibition of S6K phosphorylation induced by TGFβ (Fig. 4*E*). Collectively, these data indicated that activation of PI3K-Akt-mTOR signaling, but not the canonical Smad signaling, is required for the stimulation of vimentin protein expression by TGFβ.

To further elucidate the functional relevance of this non-canonical signaling pathway in controlling vimentin expression on ATF4-dependent activation of *Ocn* expression, we treated ROS17/2.8 reporter cells containing p6xOSE1-Luc with various kinase inhibitors. Consistent with their effects in abolishing the effect of TGFβ on vimentin production, wortmannin and rapamycin both blunted the inhibition of luciferase activity by TGFβ, whereas SB505124 did not affect it (Fig. 4*F*). Taken together, these results strengthened the finding that PI3K-Akt-mTOR signaling, but not Smad signaling, acts downstream of TGFβ to mediate the inhibition of *Ocn* transcription.

DISCUSSION

In this study, we show that TGFβ up-regulates post-transcriptionally vimentin expression in osteoblasts through a PI3K-Akt-mTOR non-canonical TGFβ pathway to inhibit osteoblast differentiation. Thus, this study defines vimentin and ATF4 as downstream mediators of TGFβ, providing two additional modulation points of this ancient and important pathway.

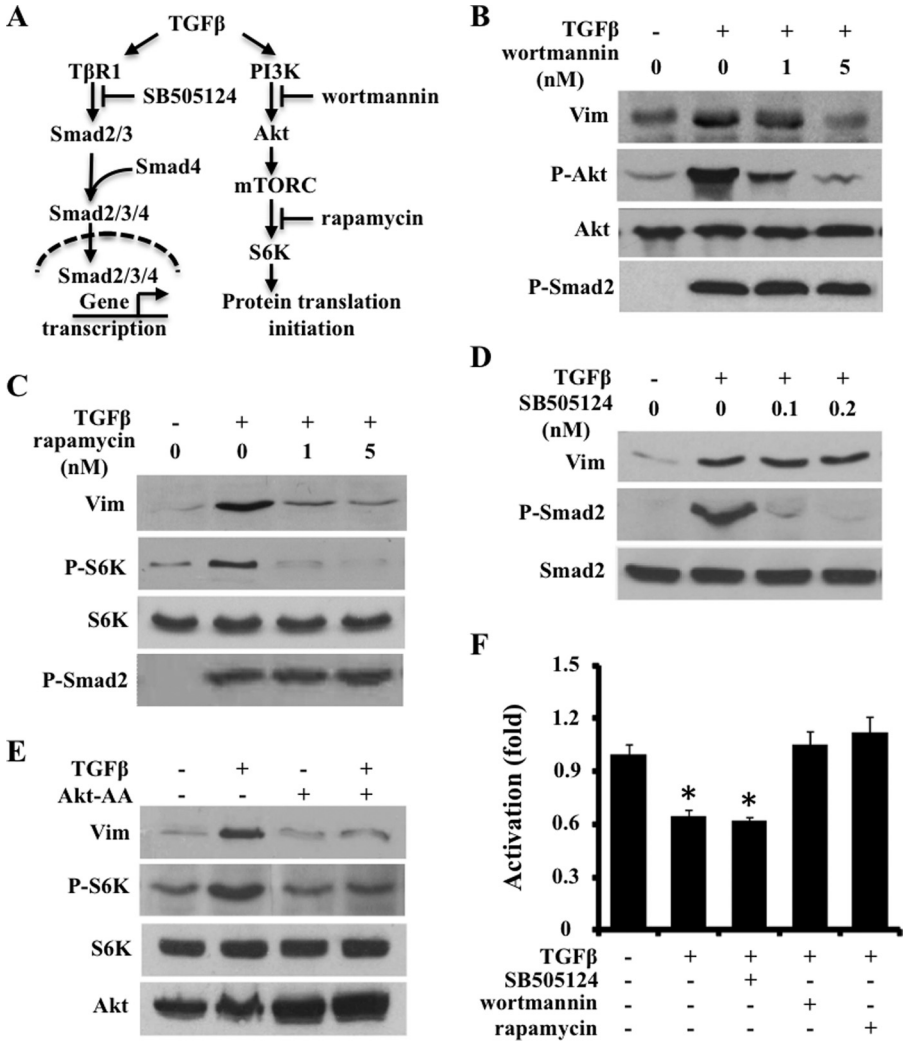

FIGURE 4. **TGFβ stimulates vimentin protein synthesis via PI3K-mTOR-Akt signaling but not Smad signaling.** *A*, schematic presentation of inhibitors that block canonical and noncanonical signaling pathways downstream of TGFβ. *B* and *C*, Western blot of ROS17/2.8 cells indicating that wortmannin (*B*) and rapamycin (*C*) dose-dependently blunted rhTGFβ1 (0.2 ng/ml) induced vimentin and phosphorylation of downstream targets Akt or S6K. *D*, Western blot analysis of ROS17/2.8 cells showing that SB505124 did not inhibit rhTGFβ1 (0.2 ng/ml) to stimulate vimentin expression. Note that SB505124 effectively inhibited Smad2 phosphorylation. *E*, Western blot analysis showing that overexpression of dominant negative form of Akt (*Akt-AA*) inhibited rhTGFβ1 (0.2 ng/ml)-induced vimentin protein level in ROS17/2.8. *F*, ATF4-dependent activation of *Ocn* transcription requires PI3K-Akt-mTOR signaling. Luciferase activity in ROS17/2.8 reporter cells containing p6xOSE1-Luc was effectively (30%) inhibited by rhTGFβ (1 ng/ml) and SB505124 (0.4 μm), which was blunted by wortmannin (5 nM) or rapamycin (5 nM). *, $p < 0.01$.

ATF4 and Vimentin as Downstream Targets of TGFβ in Osteoblasts—The finding of the monoclonal TGFβ-neutralizing antibody 1D11 to promote mechanical strength in young adult mice (30) motivated us to investigate the mechanism(s) whereby anti-TGFβ treatment promotes bone mass and fracture resistance. Here, we provided evidence that the inhibition of *Ocn* expression, ALP activity, and mineralized nodule formation by TGFβ was attenuated by 50% in $Atf4^{-/-}$ osteoblasts compared with the WT osteoblasts. Moreover, the anabolic effect of 2G7 in WT mice (a 30% increase in trabecular bone volume fraction) is completely blunted in $Atf4^{-/-}$ mice (Fig. 1). These data allow us to conclude that ATF4 is required for transmitting TGFβ signals in osteoblasts in both cultured primary cells and *in vivo*. Interestingly, TGFβ did not decrease ATF4 expression but increased vimentin protein abundance in osteoblasts and bones *in vivo* (Figs. 2 and 3), which in turn led to the suppression of ATF4 transcriptional activity. Furthermore, silencing endogenous *vimentin* by *siRNA-Vim* attenuated the effects of TGFβ (Fig. 3). Therefore, we conclude that both ATF4 and vimentin are downstream targets of TGFβ. Further investigations are necessary to confirm the *in vivo* roles that vimentin play in osteoblasts.

Studies using cell and transgenic mouse models have shown that vimentin promotes cell growth in Ras-transformed cells (41) but inhibits cell differentiation (42). Loss of vimentin ($Vim^{-/-}$) in mice results in failures of vascular adaptation, which leads to pathological conditions such as reduced renal mass (43), glial cellmalformation (44), impaired wound healing (45), decreased arterial resistance to sheer stress (46), and disturbed leukocyte homing to lymph nodes (47). It will be of interest to investigate whether all or part of these defects are attributable to the essential role that vimentin plays in transmitting the signals of TGFβ, given the versatile and essential roles that TGFβ plays in many physiological and pathological

conditions, including the ones affected in *Vim*$^{-/-}$ mice. Furthermore, vimentin is often strongly expressed in undifferentiated mesenchymal cells. Overexpressing *vimentin* in mesenchymes under its own promoter inhibited cell differentiation (48, 49). Thus, it is plausible to view TGFβ as one of the local growth factors that is required to maintain the "stemness" of mesenchymal stem cells in bone through its up-regulation of vimentin in bone. Thirdly, as an intermediate filament (IF) protein, vimentin also undergoes spatial reorganization in a variety of cell types, in response to stimulation with physiological signals, including TGFβ (data not shown). It will be important to understand the molecular basis whereby vimentin, a molecule that mostly resides in cytosol, travels into the nucleus to modulate the activity of tissue-specific transcription factors.

Analogous to the signaling axis of TGFβ-vimentin-ATF4 is that of TGFβ-Smad3-Runx2, which regulates *Ocn* transcription and osteoblast differentiation. In the latter pathway, upon TGFβ ligand stimulation, Smad3 is first phosphorylated by TGFβ receptors and then it binds to Smad4 and translocates into the nucleus, where the complex of Smad3/4 interacts with Runx2 (6), a master regulator of osteoblast differentiation (50–53). Subsequent studies demonstrated that the Smad3/4 complex also recruits histone deacetylases (HDAC) 4 and -5 to the Runx2-binding site of *Ocn* promoter to suppress *Ocn* transcription and osteoblast differentiation (54). It is currently unknown whether the vimentin-ATF4 complex can recruit additional repressors, such as HDAC family members, to the OSE1 binding site. More importantly, the relative contribution and potential interactions of TGFβ-vimentin-ATF4 and TGFβ-Smad3-Runx2 pathways remain to be studied.

The Role of PI3K-Akt-mTOR Signaling in Osteoblasts—It has previously been reported that specific inhibition of PI3K signaling with wortmannin stimulates human mesenchymal stem cells to differentiate into osteoblasts (55). Similarly, rapamycin also promotes human embryonic stem cells to differentiate into osteoblasts (56). A positive role of these kinase inhibitors of the PI3K-Akt-mTOR pathway in the regulation of osteoblast differentiation is substantiated by the evidence that both wortmannin and rapamycin blunted the inhibitory effect of TGFβ on ATF4-dependent *Ocn* transcription in ROS17/2.8 cells containing the p6xOSE1-Luc reporter (Fig. 4). At odds with these results, a low concentration (0.1 nM) of rapamycin has been shown to inhibit *Ocn* expression and osteoblast differentiation by suppressing the expression of Runx2, in primary mouse bone marrow stromal cells and MC3T3-E1 mouse osteoblastic cells (57). It is currently unknown whether these conflicting observations are a reflection of difference in cell lines, *i.e.* human *versus* mouse cell lines, or in drug concentrations. Furthermore, it needs to be further evaluated the *in vivo* relevance of the newly discovered TGFβ-PI3K-Akt-mTOR-vimentin-ATF4-Ocn axis. Regardless, our current findings represent a novel paradigm involving vimentin and ATF4 as downstream effectors of TGFβ signaling in the regulation of osteoblast differentiation.

This study does not exclude factors other than TGFβ acting as physiological upstream regulators of vimentin expression in osteoblasts. Indeed, parathyroid hormone (PTH), an important bone anabolic agent when used intermittently *in vivo*, has been reported to suppress the *de novo* biosynthesis of vimentin in human osteoblastic cells (58). Interestingly, PTH has also been shown to increase the expression and activity of ATF4 in osteoblasts (59). Thus, it is possible that PTH down-regulates vimentin expression in differentiating osteoblasts, which may counteract the action of TGFβ and lead to stimulation of ATF4's transcriptional activity and osteoblast differentiation. From this perspective, our study provides the first step toward to understanding the complexity of signaling cascades that control the anabolic action of TGFβ and PTH in bone. It is important to further determine whether vimentin is a convergent point that integrates both TGFβ and PTH signals to finely tune the differentiation process of osteoblasts.

TGFβ as a potent osteotropic factor has been extensively studied (60) and our understanding of how it regulates bone development and remodeling has continued to evolve (4, 5, 30, 61–63). It is encouraging that *in vivo* inhibition of TGFβ activity can stimulate bone formation (30). However, evaluating the long-term effects of TGFβ neutralizing antibodies on the skeleton will be important, since TGFβ promotes osteoblast proliferation and migration (63–65), two functions that are also required for bone formation. In addition, better understanding the molecular signaling pathways downstream of TGFβ should allow one to target selective molecules in osteoblast, thereby limiting off-target effects of general inhibition of TGFβ activity and the possible development of an immune response caused by the use of an antibody-based bone anabolic strategy.

Acknowledgments—We thank Dr. Florent Elefteriou and S. Kathryn Masood for critical reading of this manuscript.

REFERENCES

1. Robey, P. G., Young, M. F., Flanders, K. C., Roche, N. S., Kondaiah, P., Reddi, A. H., Termine, J. D., Sporn, M. B., and Roberts, A. B. (1987) Osteoblasts synthesize and respond to transforming growth factor-type β (TGF-β) *in vitro*. *J. Cell Biol.* **105,** 457–463
2. Lucas, P. A. (1989) Chemotactic response of osteoblast-like cells to transforming growth factor β. *Bone* **10,** 459–463
3. Pfeilschifter, J., Wolf, O., Naumann, A., Minne, H. W., Mundy, G. R., and Ziegler, R. (1990) Chemotactic response of osteoblastlike cells to transforming growth factor β. *J. Bone Miner. Res.* **5,** 825–830
4. Jian, H., Shen, X., Liu, I., Semenov, M., He, X., and Wang, X. F. (2006) Smad3-dependent nuclear translocation of β-catenin is required for TGF-β1-induced proliferation of bone marrow-derived adult human mesenchymal stem cells. *Genes Dev.* **20,** 666–674
5. Tang, Y., Wu, X., Lei, W., Pang, L., Wan, C., Shi, Z., Zhao, L., Nagy, T. R., Peng, X., Hu, J., Feng, X., Van Hul, W., Wan, M., and Cao, X. (2009) TGF-β1-induced migration of bone mesenchymal stem cells couples bone resorption with formation. *Nat. Med.* **15,** 757–765
6. Alliston, T., Choy, L., Ducy, P., Karsenty, G., and Derynck, R. (2001) TGF-β-induced repression of CBFA1 by Smad3 decreases cbfa1 and osteocalcin expression and inhibits osteoblast differentiation. *EMBO J.* **20,** 2254–2272
7. Breen, E. C., Ignotz, R. A., McCabe, L., Stein, J. L., Stein, G. S., and Lian, J. B. (1994) TGF β alters growth and differentiation related gene expression in proliferating osteoblasts in vitro, preventing development of the mature bone phenotype. *J. Cell Physiol.* **160,** 323–335
8. Centrella, M., Horowitz, M. C., Wozney, J. M., and McCarthy, T. L. (1994) Transforming growth factor-β gene family members and bone. *Endocr. Rev.* **15,** 27–39
9. Abdollah, S., Macías-Silva, M., Tsukazaki, T., Hayashi, H., Attisano, L., and Wrana, J. L. (1997) TβRI phosphorylation of Smad2 on Ser-465 and

Ser-467 is required for Smad2-Smad4 complex formation and signaling. *J. Biol. Chem.* **272,** 27678–27685
10. Massagué, J. (1998) TGF-β signal transduction. *Annu. Rev. Biochem.* **67,** 753–791
11. Bhowmick, N. A., Ghiassi, M., Bakin, A., Aakre, M., Lundquist, C. A., Engel, M. E., Arteaga, C. L., and Moses, H. L. (2001) Transforming growth factor-β1 mediates epithelial to mesenchymal transdifferentiation through a RhoA-dependent mechanism. *Mol. Biol. Cell* **12,** 27–36
12. Edlund, S., Landström, M., Heldin, C. H., and Aspenström, P. (2002) Transforming growth factor-β-induced mobilization of actin cytoskeleton requires signaling by small GTPases Cdc42 and RhoA. *Mol. Biol. Cell* **13,** 902–914
13. Frey, R. S., and Mulder, K. M. (1997) Involvement of extracellular signal-regulated kinase 2 and stress-activated protein kinase/Jun N-terminal kinase activation by transforming growth factor β in the negative growth control of breast cancer cells. *Cancer Res.* **57,** 628–633
14. Lamouille, S., and Derynck, R. (2007) Cell size and invasion in TGF-β-induced epithelial to mesenchymal transition is regulated by activation of the mTOR pathway. *J. Cell Biol.* **178,** 437–451
15. Mulder, K. M., and Morris, S. L. (1992) Activation of p21ras by transforming growth factor beta in epithelial cells. *J. Biol. Chem.* **267,** 5029–5031
16. Wilkes, M. C., Mitchell, H., Penheiter, S. G., Doré, J. J., Suzuki, K., Edens, M., Sharma, D. K., Pagano, R. E., and Leof, E. B. (2005) Transforming growth factor-β activation of phosphatidylinositol 3-kinase is independent of Smad2 and Smad3 and regulates fibroblast responses via p21-activated kinase-2. *Cancer Res.* **65,** 10431–10440
17. Yan, Z., Winawer, S., and Friedman, E. (1994) Two different signal transduction pathways can be activated by transforming growth factor β1 in epithelial cells. *J. Biol. Chem.* **269,** 13231–13237
18. Zhang, Y. E. (2009) Non-Smad pathways in TGF-β signaling. *Cell Res.* **19,** 128–139
19. Yang, X., Matsuda, K., Bialek, P., Jacquot, S., Masuoka, H. C., Schinke, T., Li, L., Brancorsini, S., Sassone-Corsi, P., Townes, T. M., Hanauer, A., and Karsenty, G. (2004) ATF4 is a substrate of RSK2 and an essential regulator of osteoblast biology; implication for Coffin-Lowry Syndrome. *Cell* **117,** 387–398
20. Hauschka, P. V. (1986) Osteocalcin: the vitamin K-dependent Ca^{2+}-binding protein of bone matrix. *Haemostasis* **16,** 258–272
21. Ducy, P., and Karsenty, G. (1995) Two distinct osteoblast-specific cis-acting elements control expression of a mouse osteocalcin gene. *Mol. Cell Biol.* **15,** 1858–1869
22. Schinke, T., and Karsenty, G. (1999) Characterization of Osf1, an osteoblast-specific transcription factor binding to a critical cis-acting element in the mouse Osteocalcin promoters. *J. Biol. Chem.* **274,** 30182–30189
23. Lian, N., Wang, W., Li, L., Elefteriou, F., and Yang, X. (2009) Vimentin inhibits ATF4-mediated osteocalcin transcription and osteoblast differentiation. *J. Biol. Chem.* **284,** 30518–30525
24. Kokkinos, M. I., Wafai, R., Wong, M. K., Newgreen, D. F., Thompson, E. W., and Waltham, M. (2007) Vimentin and epithelial-mesenchymal transition in human breast cancer–observations *in vitro* and *in vivo*. *Cells Tissues Organs* **185,** 191–203
25. Steinert, P. M., and Roop, D. R. (1988) Molecular and cellular biology of intermediate filaments. *Annu. Rev. Biochem.* **57,** 593–625
26. Wu, Y., Zhang, X., Salmon, M., Lin, X., and Zehner, Z. E. (2007) TGFbeta1 regulation of vimentin gene expression during differentiation of the C2C12 skeletal myogenic cell line requires Smads, AP-1 and Sp1 family members. *Biochim. Biophys. Acta* **1773,** 427–439
27. Katagiri, T., Yamaguchi, A., Komaki, M., Abe, E., Takahashi, N., Ikeda, T., Rosen, V., Wozney, J. M., Fujisawa-Sehara, A., and Suda, T. (1994) Bone morphogenetic protein-2 converts the differentiation pathway of C2C12 myoblasts into the osteoblast lineage. *J. Cell Biol.* **127,** 1755–1766
28. Ecarot-Charrier, B., Glorieux, F. H., van der Rest, M., and Pereira, G. (1983) Osteoblasts isolated from mouse calvaria initiate matrix mineralization in culture. *J. Cell Biol.* **96,** 639–643
29. Yang, X., Ji, X., Shi, X., and Cao, X. (2000) Smad1 domains interacting with Hoxc-8 induce osteoblast differentiation. *J. Biol. Chem.* **275,** 1065–1072
30. Edwards, J. R., Nyman, J. S., Lwin, S. T., Moore, M. M., Esparza, J., O'Quinn, E. C., Hart, A. J., Biswas, S., Patil, C. A., Lonning, S., Mahadevan-Jansen, A., and Mundy, G. R. (2010) Inhibition of TGF-β signaling by 1D11 antibody treatment increases bone mass and quality *in vivo*. *J. Bone Miner. Res.* **25,** 2419–2426
31. Wang, W., Lian, N., Li, L., Moss, H. E., Wang, W., Perrien, D. S., Elefteriou, F., and Yang, X. (2009) Atf4 regulates chondrocyte proliferation and differentiation during endochondral ossification by activating Ihh transcription. *Development* **136,** 4143–4153
32. Schreiber, E., Matthias, P., Müller, M. M., and Schaffner, W. (1989) Rapid detection of octamer binding proteins with 'mini-extracts', prepared from a small number of cells. *Nucleic Acids Res.* **17,** 6419
33. Masuoka, H. C., and Townes, T. M. (2002) Targeted disruption of the activating transcription factor 4 gene results in severe fetal anemia in mice. *Blood* **99,** 736–745
34. Dasch, J. R., Pace, D. R., Waegell, W., Inenaga, D., and Ellingsworth, L. (1989) Monoclonal antibodies recognizing transforming growth factor-β. Bioactivity neutralization and transforming growth factor β2 affinity purification. *J. Immunol.* **142,** 1536–1541
35. Pinkas, J., and Teicher, B. A. (2006) TGF-β in cancer and as a therapeutic target. *Biochem. Pharmacol.* **72,** 523–529
36. Yang, X., and Karsenty, G. (2004) ATF4, the osteoblast accumulation of which is determined post-translationally, can induce osteoblast-specific gene expression in non-osteoblastic cells. *J. Biol. Chem.* **279,** 47109–47114
37. Arcaro, A., and Wymann, M. P. (1993) Wortmannin is a potent phosphatidylinositol 3-kinase inhibitor: the role of phosphatidylinositol 3,4,5-trisphosphate in neutrophil responses. *Biochem. J.* **296,** 297–301
38. Stokoe, D., Stephens, L. R., Copeland, T., Gaffney, P. R., Reese, C. B., Painter, G. F., Holmes, A. B., McCormick, F., and Hawkins, P. T. (1997) Dual role of phosphatidylinositol-3,4,5-trisphosphate in the activation of protein kinase B. *Science* **277,** 567–570
39. Wullschleger, S., Loewith, R., and Hall, M. N. (2006) TOR signaling in growth and metabolism. *Cell* **124,** 471–484
40. DaCosta Byfield, S., Major, C., Laping, N. J., and Roberts, A. B. (2004) SB-505124 is a selective inhibitor of transforming growth factor-β type I receptors ALK4, ALK5, and ALK7. *Mol. Pharmacol.* **65,** 744–752
41. Olson, E. N., and Capetanaki, Y. G. (1989) Developmental regulation of intermediate filament and actin mRNAs during myogenesis is disrupted by oncogenic ras genes. *Oncogene* **4,** 907–913
42. Capetanaki, Y., Smith, S., and Heath, J. P. (1989) Overexpression of the vimentin gene in transgenic mice inhibits normal lens cell differentiation. *J. Cell Biol.* **109,** 1653–1664
43. Terzi, F., Henrion, D., Colucci-Guyon, E., Federici, P., Babinet, C., Levy, B. I., Briand, P., and Friedlander, G. (1997) Reduction of renal mass is lethal in mice lacking vimentin. Role of endothelin-nitric oxide imbalance. *J. Clin. Invest.* **100,** 1520–1528
44. Colucci-Guyon, E., Giménez, Y. R. M., Maurice, T., Babinet, C., and Privat, A. (1999) Cerebellar defect and impaired motor coordination in mice lacking vimentin. *Glia* **25,** 33–43
45. Eckes, B., Colucci-Guyon, E., Smola, H., Nodder, S., Babinet, C., Krieg, T., and Martin, P. (2000) Impaired wound healing in embryonic and adult mice lacking vimentin. *J. Cell Sci.* **113,** 2455–2462
46. Henrion, D., Terzi, F., Matrougui, K., Duriez, M., Boulanger, C. M., Colucci-Guyon, E., Babinet, C., Briand, P., Friedlander, G., Poitevin, P., and Lévy, B. I. (1997) Impaired flow-induced dilation in mesenteric resistance arteries from mice lacking vimentin. *J. Clin. Invest.* **100,** 2909–2914
47. Nieminen, M., Henttinen, T., Merinen, M., Marttila-Ichihara, F., Eriksson, J. E., and Jalkanen, S. (2006) Vimentin function in lymphocyte adhesion and transcellular migration. *Nat. Cell Biol.* **8,** 156–162
48. Capetanaki, Y. G., Ngai, J., and Lazarides, E. (1984) Characterization and regulation in the expression of a gene coding for the intermediate filament protein desmin. *Proc. Natl. Acad. Sci. U.S.A.* **81,** 6909–6913
49. Tapscott, S. J., Bennett, G. S., Toyama, Y., Kleinbart, F., and Holtzer, H. (1981) Intermediate filament proteins in the developing chick spinal cord. *Dev. Biol.* **86,** 40–54
50. Ducy, P., Zhang, R., Geoffroy, V., Ridall, A. L., and Karsenty, G. (1997) Osf2/Cbfa1: a transcriptional activator of osteoblast differentiation. *Cell* **89,** 747–754
51. Komori, T., Yagi, H., Nomura, S., Yamaguchi, A., Sasaki, K., Deguchi, K.,

Shimizu, Y., Bronson, R. T., Gao, Y. H., Inada, M., Sato, M., Okamoto, R., Kitamura, Y., Yoshiki, S., and Kishimoto, T. (1997) Targeted disruption of Cbfa1 results in a complete lack of bone formation owing to maturational arrest of osteoblasts. *Cell* **89,** 755–764

52. Mundlos, S., Otto, F., Mundlos, C., Mulliken, J. B., Aylsworth, A. S., Albright, S., Lindhout, D., Cole, W. G., Henn, W., Knoll, J. H., Owen, M. J., Mertelsmann, R., Zabel, B. U., and Olsen, B. R. (1997) Mutations involving the transcription factor CBFA1 cause cleidocranial dysplasia. *Cell* **89,** 773–779
53. Otto, F., Thornell, A. P., Crompton, T., Denzel, A., Gilmour, K. C., Rosewell, I. R., Stamp, G. W., Beddington, R. S., Mundlos, S., Olsen, B. R., Selby, P. B., and Owen, M. J. (1997) Cbfa1, a candidate gene for cleidocranial dysplasia syndrome, is essential for osteoblast differentiation and bone development. *Cell* **89,** 765–771
54. Kang, J. S., Alliston, T., Delston, R., and Derynck, R. (2005) Repression of Runx2 function by TGF-β through recruitment of class II histone deacetylases by Smad3. *EMBO J.* **24,** 2543–2555
55. Kratchmarova, I., Blagoev, B., Haack-Sorensen, M., Kassem, M., and Mann, M. (2005) Mechanism of divergent growth factor effects in mesenchymal stem cell differentiation. *Science* **308,** 1472–1477
56. Lee, K. W., Yook, J. Y., Son, M. Y., Kim, M. J., Koo, D. B., Han, Y. M., and Cho, Y. S. (2010) Rapamycin promotes the osteoblastic differentiation of human embryonic stem cells by blocking the mTOR, pathway and stimulating the BMP/Smad pathway. *Stem Cells Dev.* **19,** 557–568
57. Singha, U. K., Jiang, Y., Yu, S., Luo, M., Lu, Y., Zhang, J., and Xiao, G. (2008) Rapamycin inhibits osteoblast proliferation and differentiation in MC3T3-E1 cells and primary mouse bone marrow stromal cells. *J. Cell Biochem.* **103,** 434–446
58. Lomri, A., and Marie, P. J. (1990) Changes in cytoskeletal proteins in response to parathyroid hormone and 1,25-dihydroxyvitamin D in human osteoblastic cells. *Bone Miner.* **10,** 1–12
59. Yu, S., Franceschi, R. T., Luo, M., Fan, J., Jiang, D., Cao, H., Kwon, T. G., Lai, Y., Zhang, J., Patrene, K., Hankenson, K., Roodman, G. D., and Xiao, G. (2009) Critical role of activating transcription factor 4 in the anabolic actions of parathyroid hormone in bone. *PLoS One* **4,** e7583
60. Mundy, G. R. (1991) The effects of TGF-β on bone. *Ciba Found Symp.* **157,** 137–143; discussion 143–151
61. Bae, S. C., Lee, K. S., Zhang, Y. W., and Ito, Y. (2001) Intimate relationship between TGF beta/BMP signaling and runt domain transcription factor, $PEBP_2$/CBF. *J. Bone Joint Surgery* **83,** S48–S55
62. Maeda, S., Hayashi, M., Komiya, S., Imamura, T., and Miyazono, K. (2004) Endogenous TGF-β signaling suppresses maturation of osteoblastic mesenchymal cells. *EMBO J.* **23,** 552–563
63. Qiu, T., Wu, X., Zhang, F., Clemens, T. L., Wan, M., and Cao, X. (2010) TGF-β type II receptor phosphorylates PTH receptor to integrate bone remodeling signaling. *Nat. Cell Biol.* **12,** 224–234
64. Erlebacher, A., and Derynck, R. (1996) Increased expression of TGF-β2 in osteoblasts results in an osteoporosis-like phenotype. *J. Cell Biol.* **132,** 195–210
65. Erlebacher, A., Filvaroff, E. H., Ye, J. Q., and Derynck, R. (1998) Osteoblastic responses to TGF-β during bone remodeling. *Mol. Biol. Cell* **9,** 1903–1918